



## ORIGINAL ARTICLE

# SERPINE2 promotes liver cancer metastasis by inhibiting c-Cbl-mediated EGFR ubiquitination and degradation

Shiyu Zhang<sup>1,2,3,4</sup> | Xing Jia<sup>1,2,3,4</sup> | Haojiang Dai<sup>1,2,3,4</sup> | Xingxin Zhu<sup>1,2,3,4</sup> |  
 Wenfeng Song<sup>1,2,3,4</sup> | Suchen Bian<sup>1,2,3,4</sup> | Hao Wu<sup>1,2,3,4</sup> | Shinuo Chen<sup>1,2,3,4</sup> |  
 Yangbo Tang<sup>1,2,3,4</sup> | Junran Chen<sup>1,2,3,4</sup> | Cheng Jin<sup>1,2,3,4</sup> | Mengqiao Zhou<sup>1,2,3,4</sup> |  
 Haiyang Xie<sup>1,2,3,4</sup> | Shusen Zheng<sup>1,2,3,4</sup>  | Penghong Song<sup>1,2,3,4,5</sup> 

<sup>1</sup>Division of Hepatobiliary and Pancreatic Surgery, Department of Surgery, The First Affiliated Hospital, Zhejiang University School of Medicine, Hangzhou, Zhejiang, P. R. China

<sup>2</sup>National Health Commission Key Laboratory of Combined Multi-organ Transplantation, Hangzhou, Zhejiang, P. R. China

<sup>3</sup>Key Laboratory of the Diagnosis and Treatment of Organ Transplantation, Research Unit of Collaborative Diagnosis and Treatment for Hepatobiliary and Pancreatic Cancer, Chinese Academy of Medical Sciences, Hangzhou, Zhejiang, P. R. China

<sup>4</sup>Key Laboratory of Organ Transplantation, Research Center for Diagnosis and Treatment of Hepatobiliary Diseases, Hangzhou, Zhejiang, P. R. China

<sup>5</sup>State Key Laboratory for Diagnosis and Treatment of Infectious Diseases, First Affiliated Hospital, Zhejiang University School of Medicine, Hangzhou, Zhejiang, P. R. China

## Correspondence

Penghong Song and Shusen Zheng,  
 Division of Hepatobiliary and Pancreatic  
 Surgery, Department of Surgery, The First  
 Affiliated Hospital, Zhejiang University  
 School of Medicine, Hangzhou, Zhejiang  
 310003, P. R. China.

Email: [songpenghong@zju.edu.cn](mailto:songpenghong@zju.edu.cn) and  
[shusenzheng@zju.edu.cn](mailto:shusenzheng@zju.edu.cn)

## Funding information

Department of Science and Technology of  
 Zhejiang Province, Grant/Award Number:  
 2020C04003; State Key Laboratory for  
 Diagnosis and Treatment of Infectious  
 Diseases, Grant/Award Number:

## Abstract

**Background:** Liver cancer is a malignancy with high morbidity and mortality rates. Serpin family E member 2 (SERPINE2) has been reported to play a key role in the metastasis of many tumors. In this study, we aimed to investigate the potential mechanism of SERPINE2 in liver cancer metastasis.

**Methods:** The Cancer Genome Atlas database (TCGA), including DNA methylation and transcriptome sequencing data, was utilized to identify the crucial oncogene associated with DNA methylation and cancer progression in liver cancer. Data from the TCGA and RNA sequencing for 94 pairs of liver cancer tissues were used to explore the correlation between SERPINE2 expression and clinical parameters of patients. DNA methylation sequencing was used to detect the DNA methylation levels in liver cancer tissues and cells. RNA sequencing,

**List of Abbreviations:** CAF, cancer-associated fibroblast; CHX, cycloheximide; CQ, chloroquine; CT, carboxyl terminal; DMSO, dimethyl sulfoxide; DNMT, DNA-methyltransferase; ECM, extracellular matrix; EGFR, epidermal growth factor receptor; GEO, Gene Expression Omnibus; GO, Gene ontology; HIF-2 $\alpha$ , hypoxia-inducible factor-2 $\alpha$ ; HUVEC, human umbilical vein endothelial cell; IC<sub>50</sub>, lower half-maximal inhibitory concentration; ICD, intracellular domain; IP/MS, immunoprecipitation/mass spectrometry; JM, juxta membrane; PDO, patient-derived organoid; PDX, patient-derived xenograft; SERPINE2, serpin family E member 2; shRNA, short hairpin RNA; siRNA, small interfering RNA; TCGA, The Cancer Genome Atlas; TK, tyrosine kinase; UR\_CpG, unreported CpG;  $\alpha$ -SMA, alpha smooth muscle actin.

Shiyu Zhang, Xing Jia and Haojiang Dai contributed equally to this work.

This is an open access article under the terms of the [Creative Commons Attribution-NonCommercial-NoDerivs](https://creativecommons.org/licenses/by-nc-nd/4.0/) License, which permits use and distribution in any medium, provided the original work is properly cited, the use is non-commercial and no modifications or adaptations are made.

© 2024 The Authors. *Cancer Communications* published by John Wiley & Sons Australia, Ltd on behalf of SUN YAT-SEN UNIVERSITY CANCER CENTER.

zz202302; Chinese Academy of Medical Sciences, Grant/Award Number: 2019-I2M-5-030; National Natural Science Foundation of China, Grant/Award Numbers: 82070652, 81870434; Jinan Microecological Biomedicine Shandong Laboratory, Grant/Award Number: JNL-2022007B

cytokine assays, immunoprecipitation (IP) and mass spectrometry (MS) assays, protein stability assays, and ubiquitination assays were performed to explore the regulatory mechanism of SERPINE2 in liver cancer metastasis. Patient-derived xenografts and tumor organoid models were established to determine the role of SERPINE2 in the treatment of liver cancer using sorafenib.

**Results:** Based on the public database screening, SERPINE2 was identified as a tumor promoter regulated by DNA methylation. SERPINE2 expression was significantly higher in liver cancer tissues and was associated with the dismal prognosis in patients with liver cancer. SERPINE2 promoted liver cancer metastasis by enhancing cell pseudopodia formation, cell adhesion, cancer-associated fibroblast activation, extracellular matrix remodeling, and angiogenesis. IP/MS assays confirmed that SERPINE2 activated epidermal growth factor receptor (EGFR) and its downstream signaling pathways by interacting with EGFR. Mechanistically, SERPINE2 inhibited EGFR ubiquitination and maintained its protein stability by competing with the E3 ubiquitin ligase, c-Cbl. Additionally, EGFR was activated in liver cancer cells after sorafenib treatment, and SERPINE2 knockdown-induced EGFR downregulation significantly enhanced the therapeutic efficacy of sorafenib against liver cancer. Furthermore, we found that SERPINE2 knockdown also had a sensitizing effect on lenvatinib treatment.

**Conclusions:** SERPINE2 promoted liver cancer metastasis by preventing EGFR degradation via c-Cbl-mediated ubiquitination, suggesting that inhibition of the SERPINE2-EGFR axis may be a potential target for liver cancer treatment.

#### KEYWORDS

liver cancer, metastasis, DNA methylation, SERPINE2, EGFR, c-Cbl, ubiquitination

## 1 | BACKGROUND

Liver cancer remains a global health challenge, and its annual incidence is expected to exceed 1 million cases worldwide by 2025 [1]. Frequent intrahepatic and extrahepatic metastasis is the main reason for the poor therapeutic effect and prognosis of patients with liver cancer [2]. DNA methylation is an important epigenetic modification mainly mediated by DNA methylases including DNA-methyltransferase 1 (DNMT1), DNA-methyltransferase 3A (DNMT3A), and DNA-methyltransferase 3B (DNMT3B), and it plays important roles in gene regulation, structure maintenance, and other biological processes [3], including liver cancer [4].

Serpin family E member 2 (SERPINE2), also known as PN-1, has anti-serine protease activity against thrombin, urokinase, and plasminogen [5, 6]. Previous studies have demonstrated the potential role of SERPINE2 in tumor metastasis. SERPINE2 has been identified as an important marker of advanced tumor metastasis in renal cell carcinoma using single-cell sequencing [7]. In esophageal

squamous cell carcinoma, SERPINE2 promotes tumor metastasis by activating bone morphogenetic protein 4 (BMP4) [8]. Additionally, SERPINE2 has been shown to promote angiogenesis and lymphangiogenesis in oral squamous cell carcinoma [9]. However, the effect of SERPINE2 on liver cancer progression has not yet been demonstrated.

Epidermal growth factor receptor (EGFR), a member of the surface receptor tyrosine kinase family, contributes to tumor angiogenesis and metastasis [10]. More than 50% of patients with liver cancer demonstrate EGFR overexpression [11]. Wild-type EGFR can activate multiple signal transduction pathways, including the mitogen-activated protein kinase (MAPK) and janus kinase (JAK)-signal transducers and activators of transcription (STAT) signaling pathways [12]. As a classical E3 ubiquitin ligase of EGFR [13], c-Cbl mediates the ubiquitination, internalization, and lysosomal degradation of EGFR [14]. In gallbladder cancer, the inhibition of c-Cbl-mediated EGFR ubiquitination leads to activation of the EGFR signaling pathway and promotes the migration, invasion, and liver

metastasis of gallbladder cancer cells [15]. Sorafenib is widely used as a multikinase inhibitor for the treatment of patients with advanced liver cancer [16]. Previous studies have suggested that EGFR is closely related to sorafenib treatment sensitivity [17–20], but the specific mechanism is still under investigation.

In this study, we further clarified the important role of SERPINE2 in liver cancer metastasis and explored its potential molecular mechanisms, aiming to provide new therapeutic strategies for liver cancer treatment.

## 2 | MATERIALS AND METHODS

### 2.1 | Patient samples

All specimens were obtained from patients with liver cancer who underwent surgery at the First Affiliated Hospital of Zhejiang University School of Medicine, Hangzhou, China. All cases included in our study had histology indicative of liver cancer. Patients with other advanced diseases, active secondary malignancies, or those who had previously undergone any form of treatment (including radiotherapy, chemotherapy, or targeted therapy) were excluded from this study. Written informed consent was obtained from each patient. This study was approved by the Ethics Committee of the First Affiliated Hospital of Zhejiang University School of Medicine (Ethics Code: 2021-384).

Six independent cohorts were included in this study. Cohort 1 consisted of 8 paired liver cancer samples collected between April 2018 and January 2020 and were used to examine the DNA methylation level of *SERPINE2*. Cohort 2 comprised 94 pairs of liver cancer and adjacent tissues collected between June 2015 and December 2019, which were used for RNA sequencing. Cohort 3 included 6 paired liver cancer and adjacent normal tissues collected between September 2015 and June 2019, which were used to detect the protein level of *SERPINE2*. Cohort 4 consisted of 6 liver cancer tissues collected between March 2020 and November 2020, which were used to explore the relationship between *SERPINE2* and liver cancer metastasis. Cohort 5 included 113 paired liver cancer samples obtained from January 2012 to July 2017 and were used to examine the expression levels of *SERPINE2* and EGFR in liver cancer. Cohort 6 included 2 liver cancer patients collected between January 2019 and December 2019 and were used to examine the effect of *SERPINE2* expression level on sorafenib and lenvatinib sensitivity. The clinical information for patients is listed in Supplementary Tables S1–S6.

### 2.2 | Cell culture

Human liver cancer cell lines (Huh-7, SK-Hep-1, Hep 3B, and Hep G2), murine liver cancer cell line (Hepa 1-6), and HEK-293T cells were purchased from the Cell Bank of the Chinese Academy of Sciences (Shanghai, China). The human umbilical vein endothelial cell (HUVEC) was purchased from the American Type Culture Collection (Manassas, VA, USA). The human immortalized liver cell line Hep Li5 was kindly donated by Professor Lanjuan Li (State Key Laboratory for Diagnosis and Treatment of Infectious Diseases, Hangzhou, Zhejiang, China) [21]. The cancer-associated fibroblasts (CAFs) were kindly donated by Zhentao Yang (the First Affiliated Hospital of Zhejiang University School of Medicine, Hangzhou, Zhejiang, China) [22]. All cells in this study were cultured in the recommended medium (Dulbecco's Modified Eagle Medium; Thermo Fisher Scientific, Waltham, MA, USA) containing 10% fetal bovine serum (Gibco, Waltham, MA, USA) and maintained at 37°C in a 5% CO<sub>2</sub> incubator. A MycAway Plus-Color Mycoplasma Test Kit (YEASEN, Shanghai, China) was used to detect mycoplasma contamination.

### 2.3 | Cell co-culture experiments

Hepa 1-6/CAFs co-culture experiments were performed by seeding liver cancer cells ( $5 \times 10^4$ ) in the lower chamber and CAFs ( $3 \times 10^4$ ) in the upper chamber of a 24-well transwell apparatus (Corning, NY, USA). Liver cancer cells ( $3 \times 10^5$ ) were seeded in 6-cm culture dishes. After 48 h, the cell supernatant was collected and centrifuged at  $845 \times g$  for 10 min to remove cell debris. The medium was then filtered through a 0.22  $\mu$ m microwell filter membrane (BIOFIL, Guangzhou, Guangdong, China). Subsequently, the filtered medium was mixed 1:1 with fresh medium to culture the CAFs or HUVECs.

### 2.4 | Transfection and lentivirus infection

For transfection, the cells were seeded in 6-well plates at a density of  $3 \times 10^5$  cells/well. The anti-*SERPINE2* small interfering RNAs (siRNAs) were constructed by Sunya Biological (Hangzhou, Zhejiang, China) and all plasmids were constructed by REPOBIO (Hangzhou, Zhejiang, China). Liver cancer cells or HEK-293T cells were transfected with a JetPRIME transfection agent (Polyplus, Illkirch, France) according to the manufacturer's instructions. *SERPINE2*-overexpression and short

hairpin RNA (shRNA) knockdown lentivirus (Zorin Biological Company, Shanghai, China) were used to infect liver cancer cell lines, and 10  $\mu\text{g/mL}$  puromycin (Thermo Fisher Scientific, Waltham, MA, USA) was used to screen stable liver cancer cell lines. The specific sequences of the siRNAs and shRNAs are listed in Supplementary Table S7.

## 2.5 | Immunoblotting, immunoprecipitation (IP), and mass spectrometry

For immunoblotting, radioimmunoprecipitation assay lysis buffer (RIPA; Thermo Fisher Scientific, Waltham, MA, USA) with 1% protease inhibitor (Thermo Fisher Scientific, Waltham, MA, USA) was used to lyse cells for 30 min at 4°C. The protein concentration was detected using a BCA Protein Assay Kit (Pierce, Waltham, MA, USA). The extracted proteins were separated by electrophoresis at 80 V and transferred onto polyvinylidene fluoride membranes (Millipore, Billerica, MA, USA). After blocking for 1 h with western blocking buffer (Beyotime, Shanghai, China), the membranes were incubated with primary antibodies overnight at 4°C, followed by incubation with secondary antibodies for 1 h. The primary antibodies used in these experiments are listed in Supplementary Table S8. Signals were detected using chemiluminescence reagents (EZ-ECL chemiluminescence detection kit; Thermo Fisher Scientific, Waltham, MA, USA), and glyceraldehyde-3-phosphate dehydrogenase (GAPDH) was used as a control.

An endogenous IP assay was performed according to the manufacturer's instructions, using a Dynabeads Co-Immunoprecipitation Kit (Thermo Fisher Scientific, Waltham, MA, USA). Exogenous IP assays were performed using magnetic beads (Bimake, Houston, Texas, USA) precoated with anti-Flag/HA antibodies, according to the manufacturer's instructions. The magnetic beads were eluted with 50  $\mu\text{L}$  of sodium dodecyl sulfate loading buffer after washing, and the eluted protein complexes were detected by immunoblotting.

## 2.6 | Quantitative real time polymerase chain reaction (qRT-PCR)

RNA was extracted and purified using an RNA extraction kit (Shanghai Yishan Biotechnology Co. Ltd., Shanghai, China), and converted into cDNA using a reverse transcription kit (Vazyme, Nanjing, Jiangsu, China). The QuantStudio5 real-time PCR System (Thermo Fisher Scientific, Waltham, MA, USA) was utilized for performing

qRT-PCR.  $\Delta\Delta\text{Ct}$  values were used to analyze relative gene expression levels, and *GAPDH* was used as an internal control. The specific primer sequences are listed in Supplementary Table S9.

## 2.7 | Colony formation assay

Cells were seeded into 6-well plates (2,500 cells per well) and cultured for 2 weeks. Subsequently, the colonies were stained with 0.5% crystal violet (Beyotime, Shanghai, China), and the number of colonies formed was counted.

## 2.8 | Tumor sphere formation assay

For the tumor sphere assay, 1,000 cells were prepared in a serum-free medium with a single-cell suspension and then seeded in ultralow attachment 6-well plates (Corning, NY, USA) for 10 days before observing microscopically (Zeiss, Oberkochen, Germany) for sphere formation, photographing, and analysis.

## 2.9 | Cell migration and invasion assays

Filters with or without a Matrigel coating (BD Biosciences, Franklin Lakes, NJ, USA) were used for invasion or migration assays, respectively. Initially, 200  $\mu\text{L}$  of serum-free medium containing  $2 \times 10^4$  cells was added to the upper chamber, and Dulbecco's modified Eagle medium containing 10% fetal bovine serum was added to the bottom chamber. After 3 (for migration assay) or 5 (for invasion assay) days of incubation, the cells were stained with 0.5% crystal violet, photographed (Zeiss, Oberkochen, Germany), and counted.

## 2.10 | Wound-healing assay

Cells were seeded in culture inserts (Ibidi, Martinsried, Germany) for 24 h, before generating cell-free gaps by removing the culture inserts. Images were photographed using a microscope (Zeiss, Oberkochen, Germany) at 0 and 24 h after removing the culture inserts.

## 2.11 | Adhesion assay

Cell adhesion assays were performed using a Cell Adhesion Kit (BestBio, Shanghai, China). Briefly, 100  $\mu\text{L}$  of coating solution was added to 96-well plates and incubated overnight at 4°C. The coated solution was then removed,



and the plates were washed 3 times with a washing solution. The cells were seeded in 96-well plates ( $1 \times 10^5$  cells per well) and incubated for 30 min in an incubator at  $37^\circ\text{C}$ . After washing 3 times, cell-staining solution B was added and the cells were incubated at  $37^\circ\text{C}$  for 2 h. The optical density was measured at 450 nm.

## 2.12 | Trypsin digestion assay

A total of  $8 \times 10^5$  liver cancer cells were seeded in each well of 6-well plates. The next day, the cells were treated with or without 0.25% trypsin-ethylenediaminetetraacetic acid (EDTA; Gibco, Waltham, MA, USA) for 1–2 min in a cell incubator at  $37^\circ\text{C}$ . After removing the isolated cells, the remaining liver cancer cells were fixed with 4% paraformaldehyde (Beyotime, Shanghai, China) and stained with 0.5% crystal violet.

## 2.13 | HUVEC tube formation assay

Matrigel (Corning, NY, USA) was added to a pre-chilled 96-well plate and incubated at  $37^\circ\text{C}$  for 30 min until a gel formed. Subsequently,  $2 \times 10^5$  cells/mL HUVECs were suspended in the conditioned medium obtained from liver cancer cells, before seeding 100  $\mu\text{L}$  of the HUVEC suspension in 96-well plates and incubating at  $37^\circ\text{C}$  for 6–18 h. Finally, tube formation in each well was monitored using a microscope (Zeiss, Oberkochen, Germany), and the number of junctions was analyzed using ImageJ (National Institutes of Health, Bethesda, MD, USA).

## 2.14 | Dual-luciferase reporter system

A full-length mutated *SERPINE2* promoter and other related plasmids were purchased from REPOBIO (Hangzhou, Zhejiang, China). HEK-293T cells ( $1 \times 10^5$  cells/well) were seeded in 24-well plates for 1 day before transfection. The *SERPINE2* promoter plasmid and pcDNA3.1-DNMT1 plasmid (REPOBIO, Hangzhou, Zhejiang, China) were co-transfected. Mutant *SERPINE2* promoter plasmids were co-transfected with anti-DNMT1 siRNA (Supplementary Table S7), and thymidine kinase promoter-Renilla luciferase reporter plasmid (pRL-TK; REPOBIO, Hangzhou, Zhejiang, China) was transfected as a control luciferase plasmid. Forty-eight hours later, luciferase activity was measured using a Dual Luciferase Reporter Assay Kit (Promega, Madison, WI, USA).

## 2.15 | Immunofluorescence

A total of  $1 \times 10^4$  cells were seeded in confocal cell culture dishes (NEST, Wuxi, Jiangsu, China) and fixed with 4% paraformaldehyde (Beyotime, Shanghai, China). Cell cultures were incubated in the blocking buffer (0.5% TritonX-100 and 4% bovine serum albumin in phosphate-buffered saline) for 1 h. Next, the cultures were incubated with the appropriate primary antibodies (Supplementary Table S8) overnight at  $4^\circ\text{C}$ , followed by incubation with appropriate secondary antibodies (EarthOx, Millbrae, CA, USA) for 1 h. Finally, the cultures were washed 3 times before incubating with 4',6-diamidino-2-phenylindole (Sigma-Aldrich, St. Louis, MO, USA) for 5 min. Images were captured using a confocal microscope (Olympus, Tokyo, Japan).

## 2.16 | Pseudopodia staining

For the experiment of pseudopodia formation,  $1 \times 10^4$  cells were seeded in confocal cell culture dishes (NEST, Wuxi, Jiangsu, China) and fixed with 4% paraformaldehyde (Beyotime, Shanghai, China) for 15 min, and then incubated with phalloidin (Abcam, Cambridge, British) for 1 h, and then incubated with 4',6-diamidino-2-phenylindole (Sigma-Aldrich, St. Louis, MO, USA) for 5 min. Images were captured using a confocal microscope (Olympus, Tokyo, Japan).

## 2.17 | Immunohistochemistry and Masson's trichrome staining

Paraffin-embedded tissues were sectioned. Antigen retrieval (citrate buffer; Beyotime, Shanghai, China; heat-mediated epitope retrieval) was performed after dewaxing and dehydration of the sections. A blocking solution (Beyotime, Shanghai, China) was added to the sections for 30 min. Subsequently, the sections were incubated with different primary antibodies (Supplementary Table S8) overnight at  $4^\circ\text{C}$ , followed by incubation with secondary antibodies (ZSGB-BIO, Beijing, China) for 30 min. Next, the sections were subjected to diaminobenzidine color rendering and then redyed, dehydrated, and sealed. The staining intensity score was defined as 0 (no color reaction), 1 (mild reaction), 2 (moderate reaction), or 3 (intense reaction). The proportion of positive cells was defined as 0 (0%), 1 (1%–25%), 2 (26%–50%), 3 (51%–75%), or 4 (> 75%). The staining score (low, < 4; high,  $\geq 4$ ) was calculated as the intensity  $\times$  positive rate. Two independent researchers evaluated the staining scores. Masson's trichrome staining

was performed according to the instructions of Masson's trichrome staining kit (Solarbio, Beijing, China).

## 2.18 | Reagents and drugs treatment

A total of  $3 \times 10^5$  liver cancer cells were seeded in 6-cm dishes. Following 24 h of culture, decitabine ( $5 \mu\text{mol/L}$ ; MedChemExpress, Monmouth Junction, NJ, USA) was added to each well. After 48 h of treatment, the cells were collected for immunoblotting and qRT-PCR.

To explore whether SERPINE2 knockdown-induced EGFR downregulation is mediated by the proteasome or lysosomal pathway, a total of  $3 \times 10^5$  liver cancer cells were seeded in 6-cm dishes and treated with MG132 ( $10 \mu\text{mol/L}$ ; MedChemExpress, Monmouth Junction, NJ, USA) or chloroquine ( $20 \mu\text{mol/L}$ ; MedChemExpress, Monmouth Junction, NJ, USA). The liver cancer cells were collected for immunoblotting after 24 h of treatment.

Liver cancer cells transfected with control (LV-Ctrl; Zorin Biological Company, Shanghai, China) or SERPINE2 overexpression lentivirus (LV-SERPINE2; Zorin Biological Company, Shanghai, China) were seeded in 6-cm dishes ( $3 \times 10^5$  cells per well), and CHX ( $10 \mu\text{mol/L}$ ; MedChemExpress, Monmouth Junction, NJ, USA) was added to each well. The cells were collected for immunoblotting after 0, 2, 4, 8, 16, and 24 h of treatment. Liver cancer cells transfected with control (sh-Ctrl) or SERPINE2 knockdown lentivirus (sh-SERPINE2; Supplementary Table S7) were seeded in 6-cm dishes ( $3 \times 10^5$  cells per well), and sorafenib ( $5 \mu\text{mol/L}$ ; MedChemExpress, Monmouth Junction, NJ, USA) or lenvatinib ( $5 \mu\text{mol/L}$ ; MedChemExpress, Monmouth Junction, NJ, USA) was added to each well. The cells were collected for experiments after 48 h of treatment.

## 2.19 | Apoptosis analysis

Liver cancer cell apoptosis was analyzed by staining with fluorescein isothiocyanate (FITC)-labeled annexin V and propidium iodide according to the manufacturer's instructions (Dojindo Molecular Technologies, Rockville, MD, USA). The apoptosis rate was analyzed using flow cytometry (Becton, Dickinson and Company, Franklin, NJ, USA), and apoptotic populations were quantified using FlowJo-V10 software (BD Biosciences, Franklin Lakes, NJ, USA).

## 2.20 | Animal experiments

We obtained the mice used in this study from the Shanghai Experimental Animal Center of the Chinese Academy of Sciences (Shanghai, China). Mice were maintained

in a controlled pathogen-free environment with a 12-h light-dark cycle at  $24^\circ\text{C}$ , 50% humidity. At the end of the experiment, the mice were sacrificed by carbon dioxide anesthesia asphyxia. All animal experiments were approved by the Animal Care Committee of Zhejiang University (Ethics Code: 2019-1218).

For the subcutaneous xenograft model, we randomly divided BALB/c nude mice (male, 5-week-old, 20–25 g) into 4 groups: sh-Ctrl, sh-SERPINE2, sorafenib, and sh-SERPINE2 + sorafenib. Huh-7 cells transfected with sh-Ctrl and sh-SERPINE2 were injected subcutaneously into nude mice and treatment was initiated 1 week later. Sorafenib ( $30 \text{ mg/kg/day}$ ,  $1.2 \text{ mg/mL}$ , 5% dimethyl sulfoxide [DMSO]) or vehicle (5% DMSO dissolved in saline) was administered intragastrically for 4 weeks. After 4 weeks, all mice were sacrificed, and tumor tissues were collected to measure the tumor weight.

For the lung colonization model,  $2 \times 10^6$  tumor cells were injected into the tail vein for each mouse. After 2 months, all mice were sacrificed, and the lungs were carefully excised, fixed in 4% paraformaldehyde, and stained with hematoxylin and eosin. The number of nodules in the total lung lobe was counted in hematoxylin-eosin-stained images.

## 2.21 | DNA methylation and RNA sequencing

DNA methylation levels in different samples were analyzed using methyl-target sequencing (Genesky Biotechnology Inc., Shanghai, China) on a MiSeq platform (Illumina, San Diego, CA, USA). The bisulfite sequencing PCR assay was used to detect the methylation levels in different cell lines and was performed by Cosmos Wisdom Biotechnology Co., Ltd (Hangzhou, Zhejiang, China). Ninety-four pairs of liver cancer tissues and paired adjacent tissues were collected for RNA sequencing, which was performed by Applied Protein Technology Co. (Shanghai, China). SK-Hep-1 cells (si-Ctrl, si-SERPINE2) were collected for RNA sequencing, which was performed by Genedenovo Co. Ltd (Guangzhou, Guangdong, China) using a HiSeq 2500 (Illumina). Differential expression analysis was performed using DESeq2 (v3.14.0) in the R statistical environment (v3.5). Gene ontology (GO) analysis was performed using Genedenovo's online data processing platform, available at <https://www.omicsmart.com>.

## 2.22 | Public database analysis

TCGA (<http://www.cbiportal.org>) and GEO (<https://www.ncbi.nlm.nih.gov/geo/>) databases were

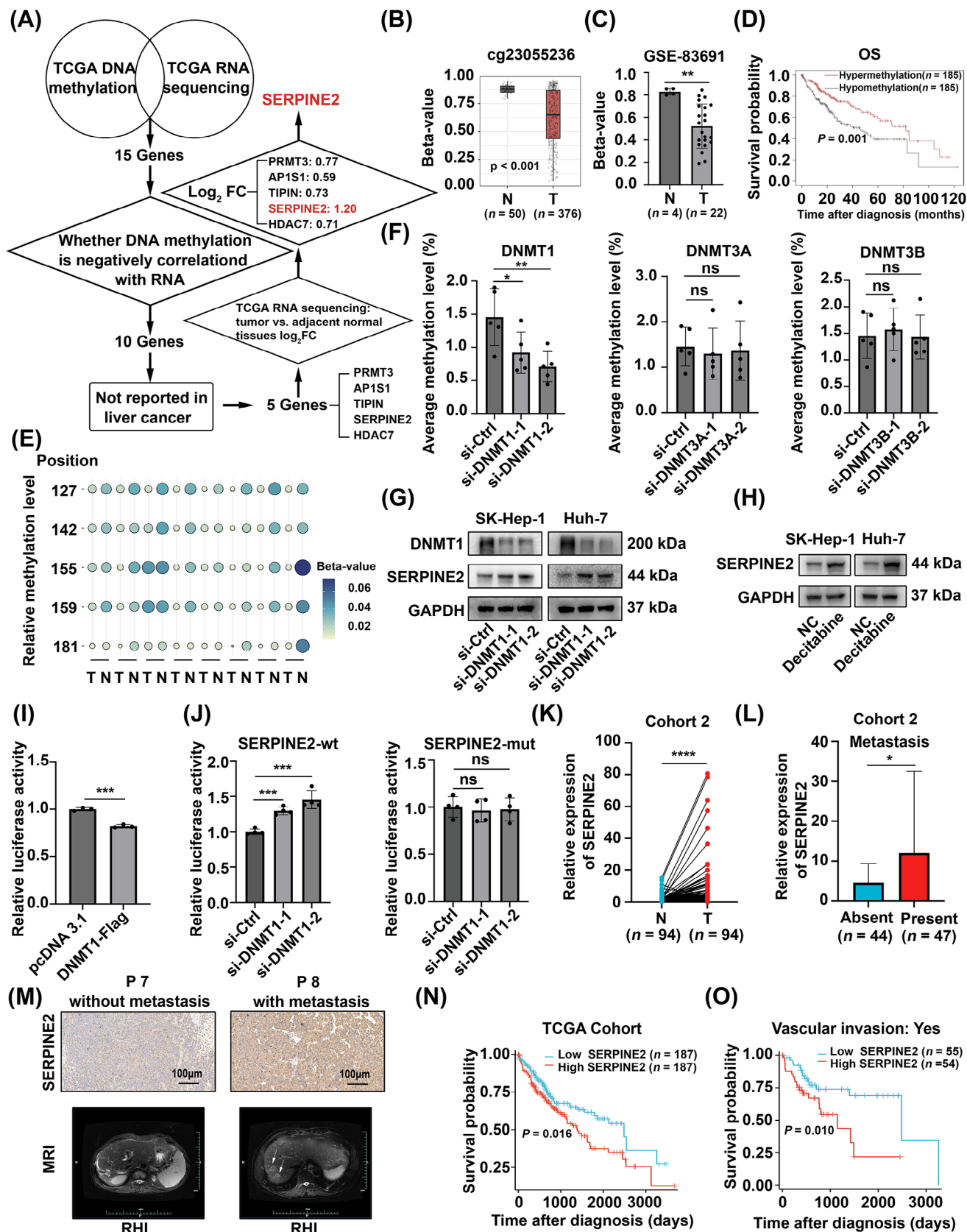


**FIGURE 1** SERPINE2 is regulated by DNA methylation and negatively correlated with patient prognosis. (A) Process of SERPINE2 screening based on TCGA database and literature review. TCGA DNA methylation: (1) The DNA methylation sites are on the promotor region; (2)  $|\text{Log}_2\text{FC}| > 0.25$ ; (3)  $\text{FDR} < 0.001$ ; (4)  $P < 0.05$  for OS and  $P < 0.05$  for DFS. TCGA RNA sequencing: (1) RNA sequencing  $\text{Log}_2\text{FC}$  has opposite signs compared to DNA methylation; (2)  $\text{FDR} < 0.05$ ; (3)  $P < 0.05$  for OS or  $P < 0.05$  for DFS. (B-C) The hypomethylation levels

used to validate the potential roles of SERPINE2 in liver cancer. EMBOSS ([https://www.ebi.ac.uk/Tools/seqstats/emboss\\_cpgplot/](https://www.ebi.ac.uk/Tools/seqstats/emboss_cpgplot/)) database was used to predict the CpG islands in the SERPINE2 promoter region. STRING (<https://string-db.org/>) database was used to predict interactions between proteins. UbiBrowser ([http://ubibrowser.bio-it.cn/ubibrowser\\_v3/](http://ubibrowser.bio-it.cn/ubibrowser_v3/)) database was used to predict the E3 ubiquitin ligase of EGFR.

## 2.23 | Patient-derived tumor organoid (PDO) and patient-derived xenograft (PDX) models

Cells derived from the liver cancer tissues of patients were extracted, and PDOs were cultured using suspended hydrogel capsule technology [23]. In brief, hydrogels consisting of 0.5% alginate (Sigma-Aldrich, St. Louis, MO, USA) and 0.25% gelatin (Sigma-Aldrich, St. Louis, MO, USA) were chosen and cross-linked using a 75 mmol/L CaCl<sub>2</sub> solution (Solarbio, Beijing, China). Before crosslinking, cells or multicellular clusters were introduced into the hydrogels. Once the hydrogels were solidified, the PDOs were successfully established and cultured for 5 days before commencing drug administration. Following that, an additional 7-day culture period was conducted. A calcein acetoxymethyl/propidium iodide (Calcein-AM/PI) double staining kit (Dojindo Molecular Technologies) was used to stain the live/dead cells. PDX experiments were approved by the Ethics Committee of the First Affiliated Hospital of Zhejiang University School of Medicine. PDX tumors in cold Dulbecco's Modified Eagle Medium (Thermo Fisher Scientific, Waltham, MA, USA) were diced into fragments with volume of 1–2 mm<sup>3</sup>. Subsequently,

each PDX tumor fragment was subcutaneously implanted into the dorsal side of NOD-scid IL2R<sup>gnull</sup> (NSG) mice.

## 2.24 | Statistical analysis

Experimental data were analyzed using GraphPad Prism 9.0 software (Graph Pad, San Diego, CA, USA). The data are presented as the means ± standard deviation. Comparisons between the 2 groups were performed using paired or unpaired Student's *t*-tests. Pearson's correlation test was used to determine the correlation between the 2 groups. All experimental conclusions were based on at least 3 independent experiments, and *P* < 0.05 was considered statistically significant.

## 3 | RESULTS

### 3.1 | SERPINE2 expression was regulated by DNA methylation

Based on the combined analysis of DNA methylation and RNA sequencing data of liver cancer patients obtained from TCGA database, *SERPINE2* was identified as an oncogene related to DNA methylation (Figure 1A). Analysis of TCGA database showed that *SERPINE2* was hypomethylated in liver cancer tissues (Supplementary Figure S1A), and 5 methylation sites were identified, all of which showed hypomethylation levels (Figure 1B, Supplementary Figure S1B). The hypomethylation level of *SERPINE2* in liver cancer tissues was further confirmed using data from the GEO database (Figure 1C, Supplementary Figure S1C), and patients

of probe cg23055236 in TCGA (B) and GSE-83691 (C) databases (mean ± SD, unpaired Student's *t*-test). (D) The OS curves showed that the hypomethylation level of *SERPINE2* predicted a poor prognosis for liver cancer patients (TCGA database). (E) DNA methylation sequencing of 8 pairs of liver cancer and paired adjacent tissues at 5 probe sites of *SERPINE2* CpG island (mean ± SD, paired Student's *t*-test). (F) The results of DNA methylation sequencing showed that DNMT1 but not DNMT3A and DNMT3B knockdown decreased the methylation level of *SERPINE2* (mean ± SD, paired Student's *t*-test). (G–H) DNMT1 knockdown (G) or stimulation with decitabine (H) promoted *SERPINE2* expression as measured by immunoblotting analysis. (I) Relative luciferase activity of the *SERPINE2* promoter after DNMT1 overexpression (mean ± SD, unpaired Student's *t*-test). (J) Relative luciferase activity of *SERPINE2* and mutant-*SERPINE2* promoter after DNMT1 knockdown (mean ± SD, unpaired Student's *t*-test). (K) The results of RNA sequencing showed that the expression of *SERPINE2* was higher in liver cancer tissues than in paired adjacent noncancerous tissues (Cohort 2, *n* = 94, mean ± SD, paired Student's *t*-test). (L) The expression of *SERPINE2* in metastatic was higher than in non-metastatic liver cancer tissues (RNA sequencing, mean ± SD, unpaired Student's *t*-test). (M) Immunohistochemical analysis was used to detect the expression of *SERPINE2* in liver cancer tissues with (patient 8) or without (patient 7) metastasis. Representative MRI images of patients with liver cancer were shown in the bottom row. White arrow: liver cancer lesions. (N) The OS curves showed that high *SERPINE2* expression predicted a poor prognosis for liver cancer (TCGA database). (O) Association between *SERPINE2* expression and the prognosis of patients with liver cancer with vascular invasion in TCGA database. \**P* < 0.05, \*\**P* < 0.01, \*\*\**P* < 0.001, \*\*\*\**P* < 0.0001. Abbreviations: DFS, disease free survival; DNMT, DNA-methyltransferase; FC, fold change; FDR, false discovery rate; MRI, magnetic resonance imaging; Mut, mutant; N, normal; NC, normal control; ns, no significance; OS, overall survival; P, patient; RHL, right hepatic lobectomy; SD, standard deviation; *SERPINE2*, serpin family E member 2; si-Ctrl, si-Control; T, tumor; TCGA, The Cancer Genome Atlas; WT, wild type.



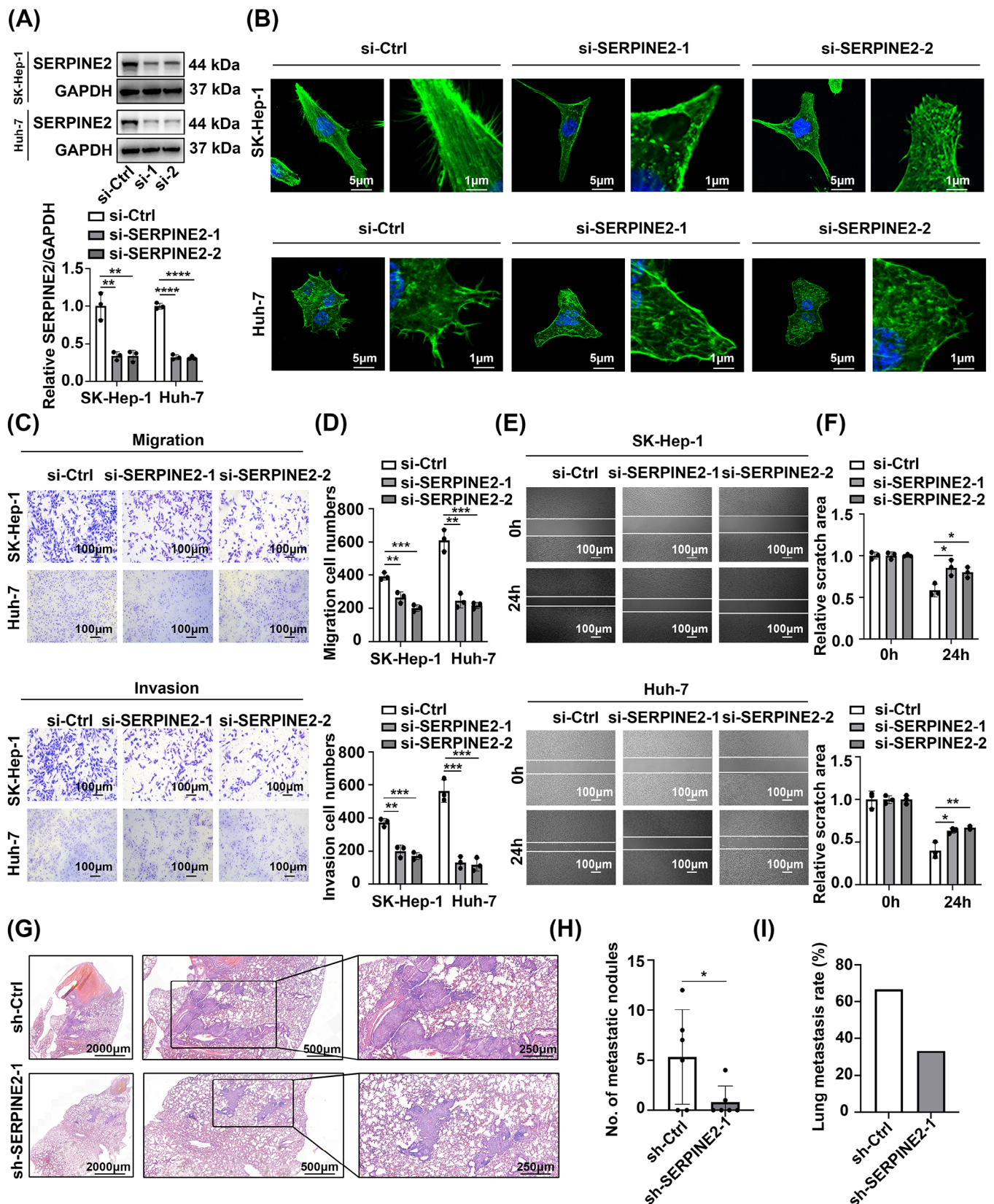


**FIGURE 2** SERPINE2 knockdown inhibits the migration and invasion of liver cancer in vitro and in vivo. (A) Immunoblotting and quantitative results of SERPINE2 expression in SERPINE2 knockdown and control liver cancer cells (means  $\pm$  SD, unpaired Student's *t*-test). (B) SERPINE2 knockdown reduced cell pseudopodia formation in SK-Hep-1 and Huh-7 liver cancer cells. (C-D) Transwell assays confirmed that SERPINE2 knockdown inhibited the migration and invasion of liver cancer cells (C). Histogram represents the numbers of cell migration

with *SERPINE2* hypomethylation tended to have a poor prognosis (Figure 1D, Supplementary Figure S1D). The *SERPINE2* promoter was evaluated using EMBOSS and an unreported CpG (UR\_CpG) island was predicted (Supplementary Figure S1E-F). Hypomethylation of *SERPINE2* in liver cancer tissues was confirmed by methyl-target DNA methylation sequencing analysis in 8 liver cancer tissue samples and paired adjacent normal tissues (Cohort 1, Figure 1E, Supplementary Figure S1G). In addition, only DNMT1 knockdown significantly inhibited the methylation level of *SERPINE2* (Figure 1F). The expression level of *SERPINE2* was upregulated in liver cancer cells following DNMT1 knockdown or stimulation with decitabine (Figure 1G-H, Supplementary Figure S1H-J). The dual-luciferase reporter system showed that DNMT1 inhibited the promoter activity of *SERPINE2* (Figure 1I). Furthermore, we constructed a mutant *SERPINE2* promoter luciferase reporter system and found that DNMT1 knockdown failed to enhance the promoter activity of the mutant *SERPINE2* promoter compared to the wide-type *SERPINE2* promoter (Figure 1J). These results suggested that *SERPINE2* is regulated by DNA methylation.

### 3.2 | High *SERPINE2* expression levels in liver cancer were closely related to the malignancy grade and prognosis

DNA methylation sequencing was used to determine the methylation levels of *SERPINE2* in different cell lines and we found that SK-Hep-1 and Huh-7 cell lines showed hypomethylation (Supplementary Figure S2A) and high *SERPINE2* protein expression levels (Supplementary Figure S2B) compared to Hep Li5 cells. RNA sequencing of liver cancer tissues and paired adjacent non-cancerous tissues (Cohort 2,  $n = 94$ ) was performed to explore the potential dysregulation of *SERPINE2* in liver cancer. The results showed that liver cancer tissues had significantly higher transcription levels of *SERPINE2* than paired adjacent normal tissues (Figure 1K), which was in agreement with the result of TCGA database analysis (Supplementary Figure S2C). Immunoblotting was performed to determine the protein levels of *SERPINE2* (Cohort 3,  $n = 6$ ), which conformed to the increased expression levels of *SERPINE2* in most liver cancer tissues (Supple-

mentary Figure S2D). Furthermore, RNA sequencing and immunohistochemical analysis (Cohort 4,  $n = 6$ ) confirmed that the expression levels of *SERPINE2* were higher in patients with liver cancer metastasis (Figure 1L-M, Supplementary Figure S2E), and early intrahepatic metastasis was observed in patients with liver cancer and high *SERPINE2* expression levels (Figure 1M, Supplementary Figure S2E). Moreover, survival analysis using data from TCGA database showed that patients with liver cancer with high *SERPINE2* expression levels tended to have a dire prognosis (Figure 1N). Of note, we also found that *SERPINE2* was highly expressed in liver cancer patients with vascular invasion (Supplementary Figure S2F), and the high *SERPINE2* expression levels predicted a poor prognosis in liver cancer patients with vascular invasion (Figure 1O). The expression levels of *SERPINE2* were significantly related with AFP levels (Supplementary Figure S2G-H) and tumor pathological stage (Supplementary Figure S2I). Taken together, our findings suggested that high *SERPINE2* expression plays an important role in promoting the malignant progression of liver cancer and is strongly associated with poor prognosis.

### 3.3 | *SERPINE2* knockdown inhibited the migratory and invasive abilities of liver cancer cells

To explore the potential mechanism by which *SERPINE2* promotes the migration and invasion of liver cancer cells, we generated *SERPINE2*-knockdown and *SERPINE2*-overexpression liver cancer cell lines using Huh-7 and SK-Hep-1 cells. The siRNA transfection efficiency was determined using fluorescence microscopy (Supplementary Figure S3A), and the knockdown and overexpression efficiencies were confirmed by immunoblotting (Figure 2A, Supplementary Figure S3B). Given that pseudopodia formation plays an important role in cancer cell motility, we sought to determine whether *SERPINE2* is involved in this process. Pseudopodia staining analysis revealed that compared to the control group, fewer pseudopodia were observed in the *SERPINE2* knockdown group (Figure 2B). Additionally, transwell and wound healing experiments showed that *SERPINE2* knockdown significantly inhibited tumor migration and

and invasion (D; mean  $\pm$  SD, unpaired Student's *t*-test). (E-F) Wound healing assays confirmed that *SERPINE2* knockdown inhibited the motility of liver cancer cells (E). Histogram represents the relative areas of the scratch (F; mean  $\pm$  SD, unpaired Student's *t*-test). (G) Representative H&E images of the lung colonization foci in the *SERPINE2*-knockdown group and its control group. (H) Number of metastatic nodules in the sh-Ctrl group and sh-*SERPINE2* group (mean  $\pm$  SD, unpaired Student's *t*-test). (I) Rate of lung metastases between the sh-Ctrl and sh-*SERPINE2* groups. \* $P < 0.05$ , \*\* $P < 0.01$ , \*\*\* $P < 0.001$ , \*\*\*\* $P < 0.0001$ . Abbreviations: SD, standard deviation; *SERPINE2*, serpin family E member 2; sh-Ctrl, sh-Control; si-Ctrl, si-Control.



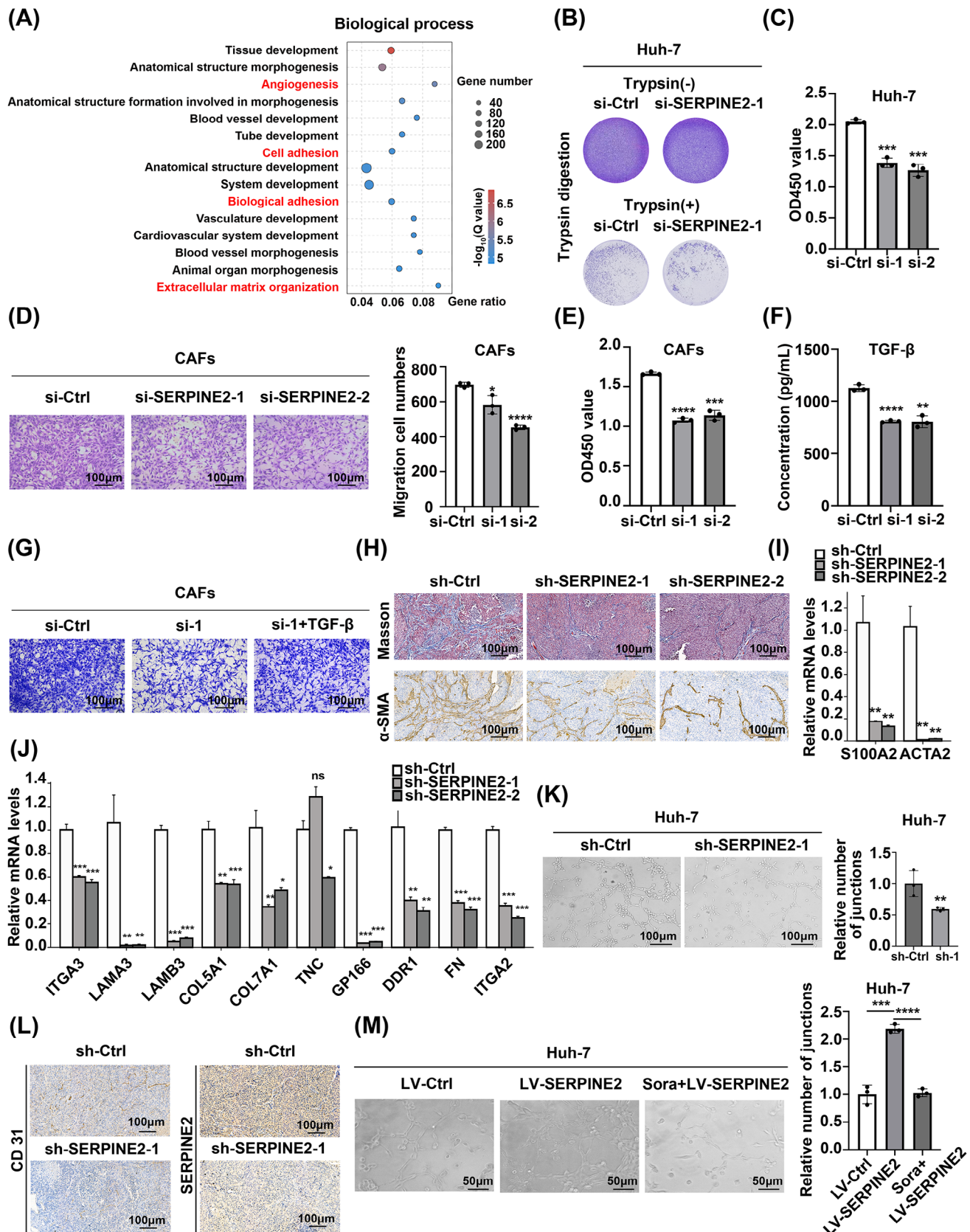


**FIGURE 3** SERPINE2 knockdown inhibits cell adhesion, ECM remodeling, and angiogenesis. (A) RNA sequencing suggested that SERPINE2 was closely related to cell adhesion, ECM, and angiogenesis. (B-C) Trypsin digestion assays and the Cell Adhesion Kit were performed to confirm that SERPINE2 knockdown inhibited cell adhesion (mean  $\pm$  SD, unpaired Student's *t*-test). (D-E) The CAFs activity was inhibited after SERPINE2 knockdown as confirmed by transwell and cell adhesion assays (mean  $\pm$  SD, unpaired Student's *t*-test). (F) TGF- $\beta$

invasion (Figure 2C-F), whereas the opposite tendency was observed in the SERPINE2-overexpression group (Supplementary Figure S3C-E). sh-SERPINE2 was constructed to explore the function of SERPINE2 in vivo (Supplementary Figure S3F), and the lung colonization experiments demonstrated that SERPINE2 knockdown reduced the size and number of metastatic nodules (Figure 2G-H), and decreased the rate of metastasis in the lung (Figure 2I). In conclusion, SERPINE2 knockdown significantly inhibited the migratory and invasive abilities of liver cancer cells both in vitro and in vivo, which may be due to the attenuation of pseudopod formation.

### 3.4 | SERPINE2 knockdown inhibited liver cancer cell adhesion, extracellular matrix (ECM) remodeling, and angiogenesis

RNA sequencing of SK-Hep-1 cells treated with si-SERPINE2 was used to explore the potential role of SERPINE2 in liver cancer metastasis (Supplementary Figure S4A). In total, 626 differentially expressed genes were detected (false discovery rate < 0.05,  $|\log_2$  fold change| > 1.2; Supplementary Figure S4B). GO analysis revealed that SERPINE2 was mainly associated with cell adhesion, ECM remodeling, and angiogenesis (Figure 3A, Supplementary Figure S4C-D). SERPINE2 knockdown significantly accelerated cell detachment after trypsin digestion in conventional cell culture (Figure 3B, Supplementary Figure S4E), implying an important role of SERPINE2 in regulating cell adhesion. To confirm this hypothesis, we performed cell adhesion assays, and the results showed that SERPINE2 knockdown significantly inhibited cell adhesion (Figure 3C, Supplementary Figure S4F). Remodeling of the ECM, mediated by CAFs, enables tumor cells to acquire stronger motility and invasion abilities [24]. To investigate the relationship between SERPINE2, ECM, and CAFs, we used a Hepa 1-6/CAFs co-culture system (Supplementary Figure S4G) and found that SERPINE2 knockdown inhibited the migration (Figure 3D) and adhesion (Figure 3E) abilities of CAFs. To further explore how SERPINE2 acti-

vates and recruits CAFs, we examined cytokines that may cause CAFs activation, such as transforming growth factor beta (TGF- $\beta$ ), C-C motif chemokine ligand 5 (CCL5), C-X-C motif chemokine ligand 12 (CXCL12), C-C motif chemokine ligand 2 (CCL2), tumor necrosis factor alpha (TNF- $\alpha$ ), and interleukin 1 beta (IL-1 $\beta$ ), in Hepa 1-6 cell supernatants and found that TGF- $\beta$  secretion was significantly decreased in SERPINE2-knockdown Hepa 1-6 cells (Figure 3F). Additionally, the CCL5 levels were slightly reduced (Supplementary Figure S4H), whereas no consistent decrease was observed for the other cytokines (Supplementary Figure S4I). Moreover, many studies have reported that tumor cells can promote the activation of CAFs by secreting TGF- $\beta$  [25–28]. We hypothesized that TGF- $\beta$  plays an important role in the activation of CAFs, and the rescue experiments with exogenous TGF- $\beta$  further confirmed that SERPINE2 knockdown inhibited the activation of CAFs, while TGF- $\beta$  treatment rescued the above inhibitory effects (Figure 3G, Supplementary Figure S4J). Therefore, the above results suggested that SERPINE2 mediated CAFs activation via TGF- $\beta$  (Supplementary Figure S4K). Masson's trichrome staining showed that the levels of collagen, the major component of ECM, were significantly reduced in SERPINE2-knockdown subcutaneous tumor tissues, and the levels of  $\alpha$ -SMA, the main marker of CAFs and angiogenesis, were also significantly decreased (Figure 3H). We also examined the expression levels of CAF-related markers (S100 calcium binding protein A2 [S100A2], and actin alpha 2 [ACTA2]) and ECM-related markers (integrin subunit alpha 3 [ITGA3], laminin subunit alpha 3 [LAMA3], and integrin subunit alpha 2 [ITGA2]) in SERPINE2-knockdown subcutaneous tumors and found that the expression levels of these markers were significantly reduced (Figure 3I-J). Additionally, the co-culture of liver cancer cells with HUVECs showed that SERPINE2 knockdown inhibited angiogenesis (Figure 3K, Supplementary Figure S4L). Immunohistochemical analysis further suggested that the expression levels of CD31 were significantly reduced in SERPINE2-knockdown subcutaneous tumors (Figure 3L). Interestingly, we found that SERPINE2 overexpression significantly promoted angiogenesis, which was attenuated by sorafenib treatment

secretion level was decreased in SERPINE2 knockdown Hepa 1-6 cells. (G) TGF- $\beta$  treatment rescued CAFs activity in the SERPINE2-knockdown group, as determined by the transwell assay. (H) Masson and immunohistochemical staining of  $\alpha$ -SMA in xenograft tumors of SERPINE2-knockdown group and control group. (I-J) mRNA levels of CAF-related genes (I) and ECM-related genes (J) in SERPINE2 knockdown xenograft tumors (mean  $\pm$  SD, unpaired Student's *t*-test). (K) An angiogenesis assay confirmed that SERPINE2 knockdown inhibited angiogenesis, and the histogram represented the relative number of junctions (mean  $\pm$  SD, unpaired Student's *t*-test). (L) Immunohistochemical staining of CD31 and SERPINE2 in xenograft tumors of SERPINE2-knockdown group and control group. (M) Sorafenib inhibited SERPINE2-induced proangiogenesis. \**P* < 0.05, \*\**P* < 0.01, \*\*\**P* < 0.001, \*\*\*\**P* < 0.0001. Abbreviations:  $\alpha$ -SMA, alpha smooth muscle actin; CAF, cancer-associated fibroblast; ECM, extracellular matrix; LV, lentivirus; ns, no significance; SD, standard deviation; SERPINE2, serpin family E member 2; sh-Ctrl, sh-Control; si-Ctrl, si-Control; Sora, sorafenib.



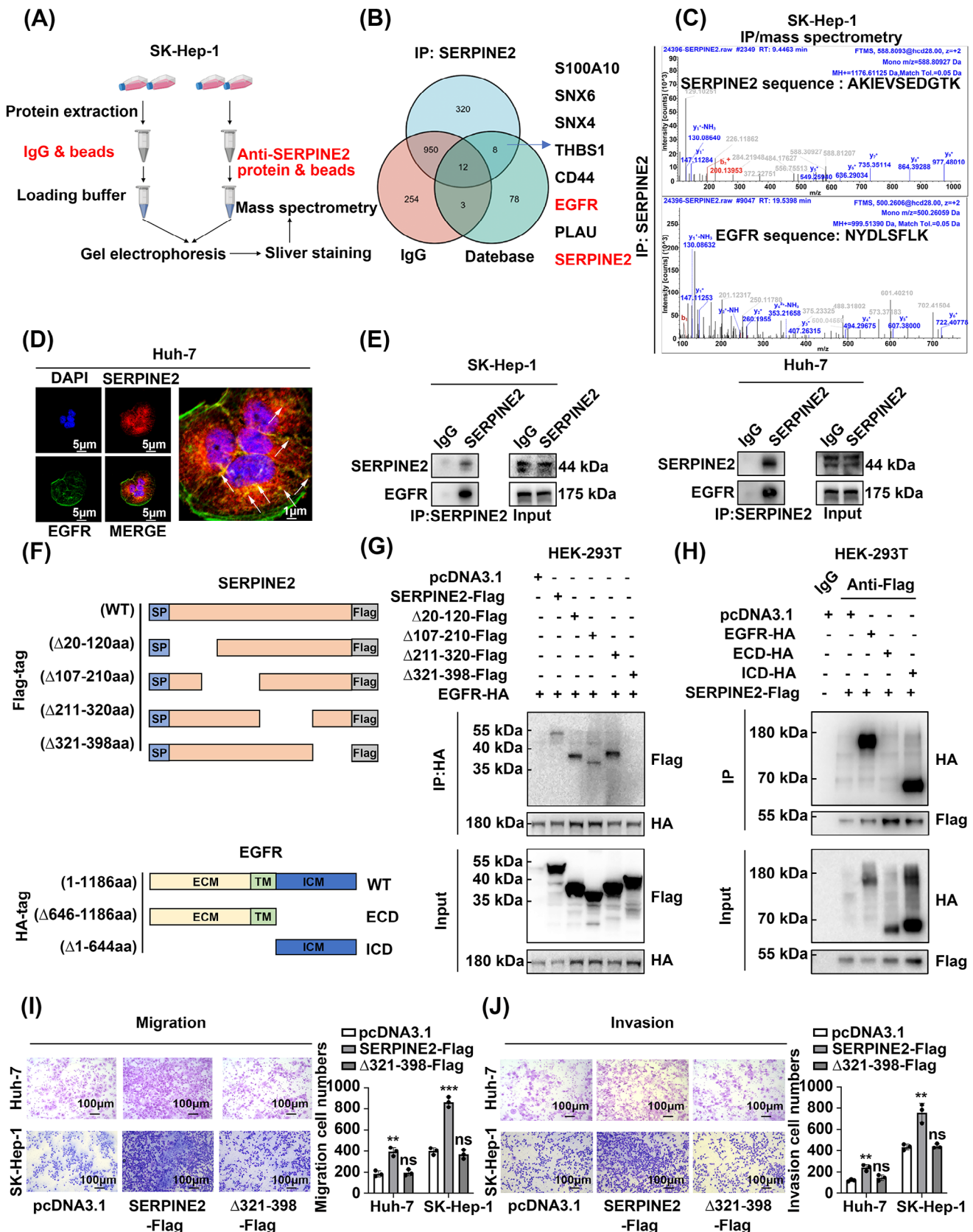


**FIGURE 4** SERPINE2 combines with EGFR to promote liver cancer metastasis. (A-C) EGFR was identified as a potential SERPINE2-binding protein by IP/MS analysis. Flowchart of IP/MS analysis showed in A. Seven candidate genes that interacted with SERPINE2 were screened by IP/MS and STRING database analysis (B). Secondary mass spectra of IP/MS analysis showed in C. (D) Immunofluorescence assay for the colocalization of SERPINE2 and EGFR. (E) Immunoblotting analysis of the endogenous interaction

(Figure 3M, Supplementary Figure S4M). Taken together, these results suggested that SERPINE2 promotes tumor metastasis by increasing cell adhesion, ECM remodeling, and angiogenesis.

### 3.5 | EGFR was identified as an interacting protein of SERPINE2

To identify the SERPINE2-associated proteins and explore the potential molecular mechanisms of SERPINE2 in liver cancer metastasis, IP/mass spectrometry analysis (Figure 4A) combined with data from the STRING database identified 7 potential SERPINE2-interacting proteins, including EGFR (Figure 4B-C). Finally, we focused on EGFR as the key SERPINE2-associated protein because it is a powerful oncogene that promotes tumor progression. The colocalization and binding of SERPINE2 and EGFR in liver cancer cells were further verified by immunofluorescence (Figure 4D) and IP assays (Figure 4E), respectively. We explored the relationship between SERPINE2 and EGFR by generating truncation constructs (Figure 4F). The IP experiment showed that compared to other SERPINE2 truncations, Flag-SERPINE2-Δ321-398 had a weaker ability to bind to EGFR (Figure 4G). Furthermore, domain mapping of EGFR indicated that SERPINE2 interacted with the intracellular domain (ICD, 645-1186 aa) of EGFR (Figure 4H). Additionally, compared with wild-type SERPINE2, the truncated mutant protein, Flag-SERPINE2-Δ321-398 failed to promote liver cancer metastasis (Figure 4I-J). Taken together, these results suggested that the interaction between SERPINE2 and EGFR affects liver cancer metastasis.

### 3.6 | SERPINE2 maintained EGFR protein stability by protecting EGFR from lysosomal degradation

We further explored the relationship between SERPINE2 and EGFR and found that SERPINE2 overexpression did not significantly change *EGFR* mRNA levels (Figure 5A, Supplementary Figure S5A) but significantly increased EGFR protein levels (Figure 5B, Supplementary Figure S5B), suggesting possible post-transcriptional regulation of

EGFR by SERPINE2. We also examined the downstream signaling pathway of EGFR, and the results showed that SERPINE2 overexpression caused activation of the STAT3 and ERK1/2 pathways. Conversely, the STAT3 and ERK1/2 pathways were inhibited after SERPINE2 knockdown in Huh-7 and SK-Hep-1 cells (Figure 5B, Supplementary Figure S5B). We next performed immunohistochemical staining, which revealed a significant positive correlation between SERPINE2 and EGFR expression levels (Cohort 5, Figure 5C, Supplementary Figure S5C). Immunofluorescence analysis further confirmed that the EGFR expression levels decreased after SERPINE2 knockdown (Supplementary Figure S5D). SERPINE2 knockdown inhibited cell migration and adhesion, which were fully rescued by EGFR overexpression (Figure 5D-E, Supplementary Figure S5E-G). Additionally, we found that, of the truncation mutants tested, only Flag-SERPINE2-Δ321-398 inhibited EGFR activation caused by SERPINE2 overexpression (Figure 5F). Taken together, these results suggested that the stimulatory effect of SERPINE2 on liver cancer metastasis depends on its interaction with EGFR.

Given the lack of the effect of SERPINE2 overexpression on EGFR transcription in Huh-7 and SK-Hep-1 cells, we hypothesized that SERPINE2 regulates EGFR degradation. Next, we determined the protein stability of EGFR and found that SERPINE2 overexpression significantly extended the half-life of EGFR in liver cancer cells (Figure 5G-H, Supplementary Figure S6A). Additionally, we found that the downregulation of EGFR induced by SERPINE2 knockdown was inhibited by the lysosomal inhibitor chloroquine, but not by the proteasome inhibitor MG132 (Figure 5I, Supplementary Figure S6B-C). EGFR ubiquitination is essential for EGFR stability. SERPINE2 overexpression reduced EGFR ubiquitination in liver cancer cells (Figure 5J, Supplementary Figure S6D), which was further confirmed in HEK-293T cells (Figure 5K). Conversely, SERPINE2 knockdown promoted EGFR ubiquitination in SK-Hep-1 and Huh-7 cells (Figure 5L, Supplementary Figure S6E). Furthermore, the ubiquitin assay provided compelling evidence that SERPINE2 could remove K63-linked ubiquitin chains from EGFR in HEK-293T cells (Figure 5M). In conclusion, SERPINE2 maintains EGFR protein stability by inhibiting EGFR ubiquitination and lysosomal degradation.

between SERPINE2 and EGFR after IP in SK-Hep-1 and Huh-7 cells. (F) SERPINE2 and EGFR truncations were constructed according to UniProt. (G) The interaction between different SERPINE2 truncations and EGFR in HEK-293T cells was evaluated by IP assays. (H) The interaction between different truncations of EGFR and SERPINE2 in HEK-293T cells was evaluated by IP assays. (I-J) Transwell assays confirmed that Flag-SERPINE2-Δ321-398 could not promote the migration (I) and invasion (J) of liver cancer cells. \*\**P* < 0.01, \*\*\**P* < 0.001. Abbreviations: ECD, extracellular domain; EGFR, epidermal growth factor receptor; ICD, intracellular domain; IP, immunoprecipitation; MS, mass spectrum; ns, no significance; SERPINE2, serpin family E member 2; WT, wild type.

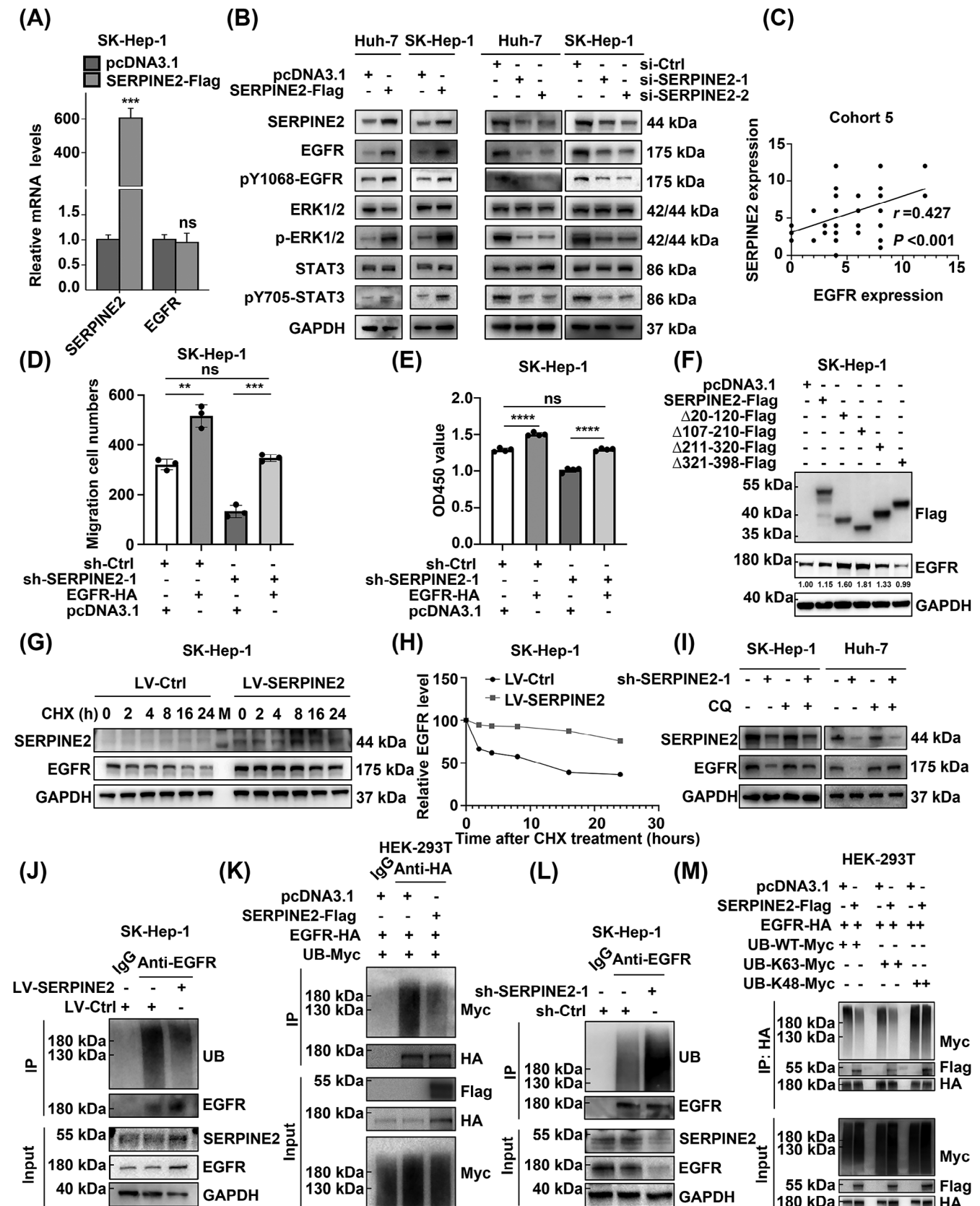


**FIGURE 5** SERPINE2 maintains EGFR stability and activates EGFR downstream pathways by inhibiting lysosomes. (A) The mRNA level of EGFR after SERPINE2 overexpression was detected by qRT-PCR. (B) The protein levels of EGFR and its downstream signaling pathways were determined by immunoblotting after SERPINE2 overexpression (left) or knockdown (right). (C) Immunohistochemical analysis was used to explore the relationship between SERPINE2 and EGFR (Pearson's correlation test). (D-E) Ectopic expression of EGFR



### 3.7 | SERPINE2 interacted with EGFR to inhibit c-Cbl-mediated EGFR ubiquitination and degradation

E3 ubiquitin ligases are the enzymes responsible for transferring ubiquitin molecules to specific target proteins. The UbiBrowser database was used to explore the related upstream E3 ubiquitin ligase of EGFR, and 12 previously reported E3 ubiquitin ligases, including c-Cbl, were identified (Figure 6A). The STRING database further confirmed that c-Cbl was the only E3 ubiquitin ligase among the top 10 EGFR-binding genes (Supplementary Figure S7A). Therefore, we investigated the role of c-Cbl in regulating EGFR expression in liver cancer cells. c-Cbl overexpression decreased EGFR protein levels in liver cancer cells (Supplementary Figure S7B). The binding of EGFR and c-Cbl in HEK293T cells (Figure 6B) and liver cancer cells (Supplementary Figure S7C) were further verified using IP assays. Immunofluorescence analysis suggested that c-Cbl colocalized with EGFR, mainly in the intracellular region (Supplementary Figure S7D). c-Cbl overexpression increased EGFR ubiquitination in liver cancer cells (Supplementary Figure S7E). EGFR overexpression induced the activation of cell motility and adhesion, whereas c-Cbl overexpression inhibited these effects (Supplementary Figure S7F-G). We confirmed that the c-Cbl interacted with the ICD of EGFR in HEK293T cells (Figure 6C). We further found that c-Cbl mainly interacted with the carboxyl terminal (CT) of the ICD (Figure 6D-E). Moreover, previous studies have reported that c-Cbl is directly recruited to Tyr1045 of ICD for EGFR ubiquitination [14, 29]. We constructed an EGFR mutant plasmid (EGFR-HA-Y1045F) and found that the binding ability of c-Cbl to the EGFR mutant plasmid was decreased (Figure 6F). The c-Cbl-mediated ubiquitination of EGFR was also impaired when Tyr1045 of ICD was mutated (Figure 6G).

To further clarify the role of SERPINE2 in c-Cbl-mediated EGFR regulation, we overexpressed SERPINE2 and found that it promoted EGFR expression, but did not affect c-Cbl (Supplementary Figure S7H). An IP-Flag

assay showed that the CT, juxta membrane (JM), and tyrosine kinase (TK) domains of ICD interacted with SERPINE2, with the CT domain exhibiting the strongest binding affinity (Figure 6H). The Y1045F mutation in ICD inhibited the interaction between SERPINE2 and EGFR (Figure 6I). SERPINE2 overexpression significantly inhibited the interaction between EGFR and c-Cbl in liver cancer cells (Figure 6J, Supplementary Figure S7I). In addition, the binding between c-Cbl and EGFR was gradually suppressed by SERPINE2 in HEK293T cells (Figure 6K). Moreover, overexpression of SERPINE2 significantly rescued c-Cbl-mediated EGFR ubiquitination (Figure 6L, Supplementary Figure S7J). Overall, these results suggested that SERPINE2 is essential for the inhibition of c-Cbl-mediated EGFR ubiquitination and degradation.

### 3.8 | SERPINE2 knockdown sensitized liver cancer to sorafenib in vitro and in vivo

Sorafenib is a first-line treatment for advanced liver cancer and previous studies have shown that EGFR-targeted therapy enhances the efficacy of sorafenib in liver cancer cells [17, 30, 31]. The sensitivity of liver cancer cells to sorafenib can be reduced by activating the ras proto-oncogene (RAS)/ raf proto-oncogene (Raf)/mitogen-activated protein kinase kinase (MEK)/extracellular signal-regulated kinase (ERK) signaling pathway, which is a downstream signaling pathway of EGFR [32]. Thus, we speculated that SERPINE2-knockdown-induced EGFR downregulation contributes to the sensitivity of liver cancer cells to sorafenib treatment. We found that EGFR was activated after sorafenib treatment of Huh-7 and SK-Hep-1 cells (Figure 7A, Supplementary Figure S8A), and knockdown of SERPINE2 in liver cancer cells resulted in a consistently lower half-maximal inhibitory concentration (IC<sub>50</sub>) after sorafenib treatment than in the control group (Figure 7B; Supplementary Figure S8B). Transwell, tumor sphere, and colony-formation assays demonstrated that the combination of SERPINE2 knockdown and sorafenib treatment

reversed SERPINE2 knockdown-induced inhibition of metastasis in SK-Hep-1 cells, as detected using cell migration (D) and adhesion assays (E; mean  $\pm$  SD, unpaired Student's *t*-test). (F) EGFR protein levels were measured by immunoblotting in SK-Hep-1 cells transfected with different SERPINE2 truncations. (G) SERPINE2 overexpression extended the half-life of EGFR. SK-Hep-1 cells were transfected with the indicated lentivirus and treated with CHX (10  $\mu$ g/mL) for the indicated times. (H) Quantification of CHX assay in G. (I) Immunoblotting detected the expression of EGFR in SERPINE2 knockdown liver cancer cells with or without chloroquine treatment (20  $\mu$ mol/L). (J-L) SERPINE2 affected EGFR ubiquitination in SK-Hep-1 (J and L) and HEK-293T cells (K) as measured by ubiquitin analysis. (M) HEK-293T cells were co-transfected with UB-Myc (UB-WT-Myc, UB-K63-Myc, or UB-K48-Myc) and EGFR-HA with or without SERPINE2-Flag. Immunoblotting was used to detect the EGFR ubiquitination level. \*\**P* < 0.01, \*\*\**P* < 0.001, \*\*\*\**P* < 0.0001. Abbreviations: CHX, cycloheximide; CQ, chloroquine; EGFR, epidermal growth factor receptor; IP, immunoprecipitation; LV, lentivirus; M, marker; ns, no significance; qRT-PCR, quantitative real time polymerase chain reaction; SERPINE2, serpin family E member 2; sh-Ctrl, sh-Control; si-Ctrl, si-Control; UB, ubiquitin.



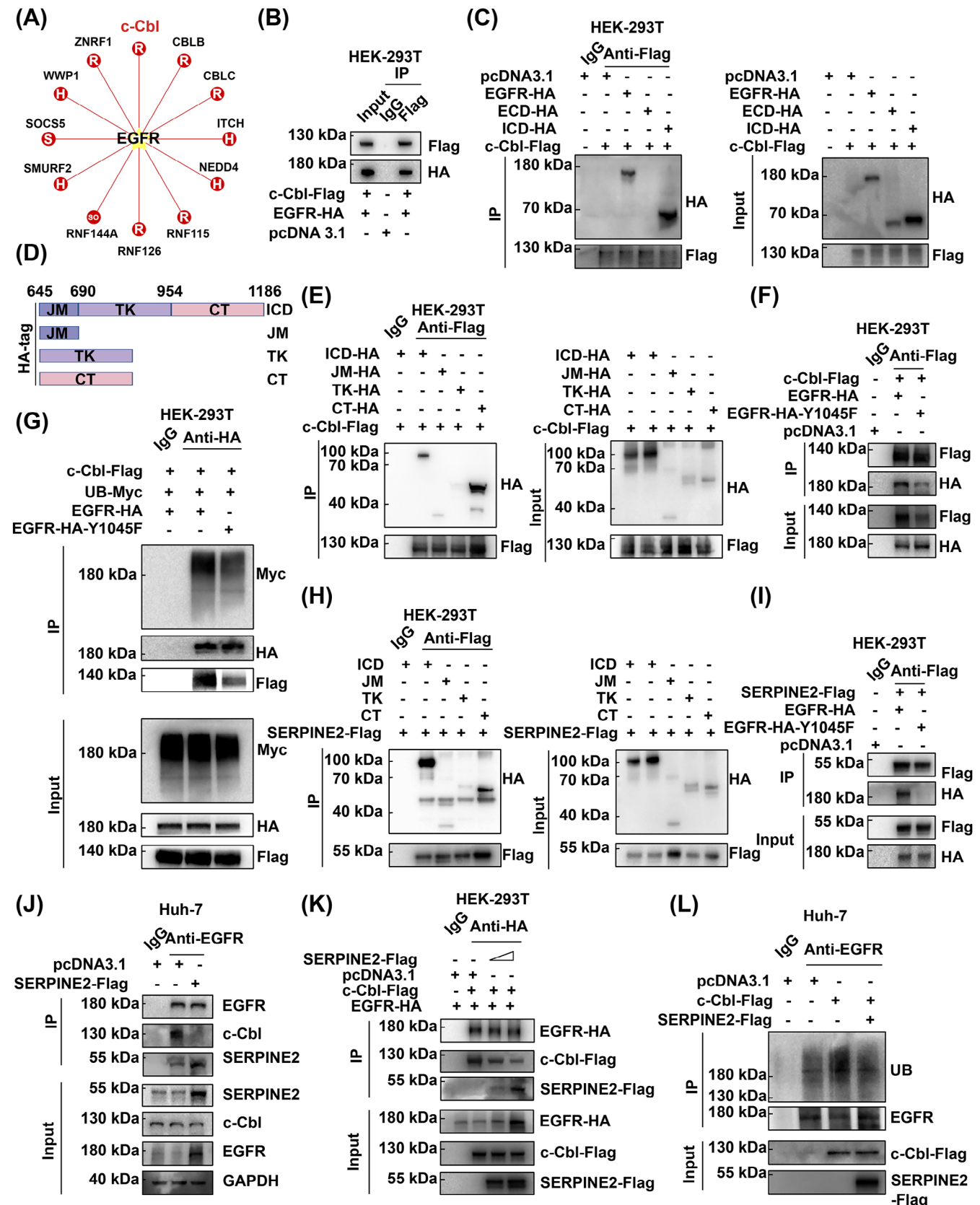


**FIGURE 6** SERPINE2 interacts with EGFR to inhibit c-Cbl-mediated EGFR ubiquitination and degradation. (A) The UbiBrowser database was used to analyze the upstream E3 ubiquitin ligase of EGFR. (B) Immunoblotting analysis of the exogenous interaction between c-Cbl and EGFR in HEK-293T cells. (C) The interaction between different truncations of EGFR and c-Cbl in HEK-293T cells was evaluated by IP assay. (D) The EGFR ICD truncations were constructed according to UniProt. (E) The interaction between different truncations of EGFR

was significantly more effective than sorafenib treatment alone (Figure 7C-E, Supplementary Figure S8C-D). Furthermore, the results of flow cytometry analysis suggested that when SERPINE2 knockdown was combined with sorafenib treatment, apoptosis of liver cancer cells was significantly increased (Supplementary Figure S8E). The liver cancer xenograft model further supported our *in vitro* results, showing that the volume and weight of tumors in the SERPINE2-knockdown + sorafenib and sorafenib groups were lower than those in the SERPINE2-knockdown and control groups. Moreover, SERPINE2 knockdown combined with sorafenib treatment inhibited tumor growth more significantly than sorafenib alone (Figure 7F-G), and the immunohistochemical analysis results further suggested that the expression levels of Ki-67 were significantly reduced in the SERPINE2-knockdown + sorafenib group (Figure 7H). Additionally, 2 patient-derived liver cancer tissues were collected (Figure 7I) and divided into high- and low-SERPINE2 expression groups (Figure 7J). The results of the immunohistochemical analysis showed that the levels of SERPINE2 in PDXs were partially upregulated after sorafenib treatment (Supplementary Figure S8F), suggesting that SERPINE2 plays an important role in the response of liver cancer cells to sorafenib. PDXs and PDOs from patients (Cohort 6) with low SERPINE2 expression levels were more sensitive to sorafenib (Figure 7K-L). Therefore, SERPINE2 knockdown contributed to the sensitization of patients with liver cancer to sorafenib treatment. To verify the effect of SERPINE2 on sorafenib treatment through regulating EGFR, we first constructed siRNA-3 to target the 3'-untranslational region (UTR) in human SERPINE2 mRNA (Supplementary Figure S8G). We exogenously overexpressed SERPINE2 in SERPINE2-knockdown cells and found that SERPINE2 knockdown increased sorafenib sensitivity, and this was rescued by Flag-SERPINE2 but not Flag-SERPINE2-Δ321-398 (Supplementary Figure S8H-J). The tyrosine kinase inhibitor lenvatinib is another first-line therapeutic agent for patients with advanced liver cancer. However, feedback activation of the EGFR-protein activated kinase 2 (PAK2)-ERK5 signaling pathway after lenvatinib treatment reduces the sensitivity of liver cancer cells to lenvatinib [33]. To determine the potential role of

SERPINE2 in liver cancer treatment, we further attempted to explore whether SERPINE2 could regulate the efficacy of lenvatinib and found that SERPINE2 knockdown in SK-Hep-1 and Huh-7 cells resulted in a reduced IC<sub>50</sub> value after lenvatinib treatment, as compared with the control cells (Supplementary Figure S9A). Furthermore, the results of transwell and colony-formation assays demonstrated that SERPINE2 knockdown significantly enhanced the inhibitory effect of lenvatinib on tumor metastasis and growth (Supplementary Figure S9B-C). Moreover, patients with low levels of SERPINE2 expression showed a higher sensitivity to lenvatinib in the PDO model (Supplementary Figure S9D). Based on these results, we propose the hypothetical model shown in Figure 8.

## 4 | DISCUSSION

In the current study, we conducted an in-depth exploration of the effect of SERPINE2 on liver cancer metastasis through *in vitro* and *in vivo* experiments and clinical specimen analyses. As a result, we identified an important tumor metastasis-promoting gene regulated by DNA methylation in liver cancer and revealed that SERPINE2 regulated EGFR ubiquitination, maintained EGFR stability, and promoted liver cancer metastasis by competing with c-Cbl. Collectively, our results suggest that targeting the SERPINE2-EGFR axis may provide a basis for novel therapeutic strategies against liver cancer metastasis.

Based on the combined analysis of TCGA and GEO databases, SERPINE2 was found to be closely related to DNA methylation. However, the role of SERPINE2 in the metastasis of liver cancer remains unclear. Our study demonstrated that SERPINE2 expression levels were significantly higher in liver cancer tissues compared with normal tissues and its levels were negatively correlated with the prognosis of patients with liver cancer. SERPINE2 significantly promoted liver cancer metastasis both *in vitro* and *in vivo*.

As a form of DNA modification, DNA methylation can alter genetic performance and regulate gene expression without changing the DNA sequence [34]. Disruption of DNA methylation is associated with multiple common

ICD and c-Cbl in HEK-293T cells was evaluated by IP assays. (F) c-Cbl bound to the Tyr1045 of EGFR ICD by IP assay. (G) The c-Cbl-mediated ubiquitination of EGFR was impaired when Tyr1045 of the ICD was mutated by ubiquitin assays. (H) The interaction between different truncations of EGFR ICD and SERPINE2 in HEK-293T cells was evaluated by IP assays. (I) EGFR-HA-Y1045F impaired the interaction between SERPINE2 and EGFR. (J-K) The ectopic expression of SERPINE2 affected endogenous (J) and exogenous (K) interactions between c-Cbl and EGFR. (L) Ectopic expression of SERPINE2 inhibited c-Cbl-induced EGFR ubiquitination in Huh-7 cells as measured by ubiquitin analysis. Abbreviations: c-Cbl, c-casitas B-lineage lymphoma; CT, carboxyl terminal; EGFR, epidermal growth factor receptor; ICD, intracellular domain; IP, immunoprecipitation; JM, juxtamembrane domain; SERPINE2, serpin family E member 2; TK, tyrosine kinase domain; UB, ubiquitin.

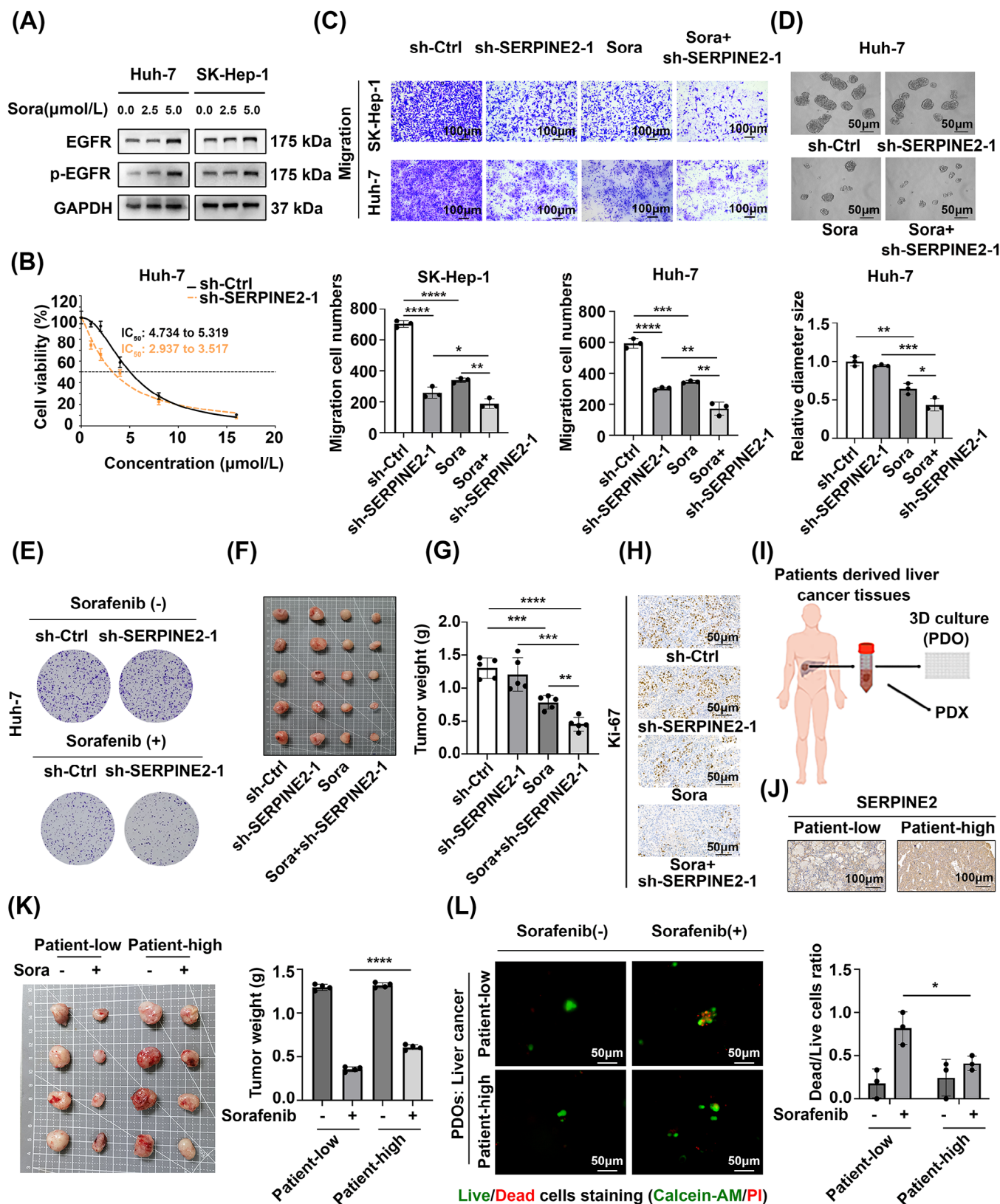


**FIGURE 7** SERPINE2 knockdown increases the sensitivity of liver cancer cells to sorafenib treatment. (A) The results of immunoblotting showed that EGFR was activated after sorafenib (Sora) treatment. (B) IC<sub>50</sub> of sorafenib in the SERPINE2-knockdown group and its control group. (C) Cell migration assays confirmed that SERPINE2 knockdown enhanced the inhibitory effect of sorafenib (Sora) on tumor cell motility (mean ± SD, unpaired Student's *t*-test). (D-E) SERPINE2 knockdown enhanced the inhibitory effect of sorafenib (Sora) on



human diseases, including cancer [35]. In general, tumors are characterized by dysregulated DNA methylation, which mainly targets the CpG islands [36]. Our previous study explored the relationship between CpG island methylation and the expression of the tumor suppressor ASGR1, mediated by DNA methylase [37]. In this study, we identified an UR\_CpG island in the promoter region of *SERPINE2* and found that the UR\_CpG island was

significantly hypomethylated in liver cancer tissues, similar to the findings from TCGA database. Additionally, using methyl-target sequencing, we confirmed that the expression of *SERPINE2* was regulated by DNA methylation, and DNMT1 was further confirmed as the most critical methylase mediating this process.

The ECM is an interstitial element in biological tissues or organs and it plays a crucial role in all biological

tumor cell growth, as confirmed by tumor sphere (D) and colony formation assays (E; mean  $\pm$  SD, unpaired Student's *t*-test). (F) Photographs of subcutaneous tumors in the *SERPINE2*-knockdown group, sorafenib group, *SERPINE2*-knockdown + sorafenib group, and control group. (G) The weight of subcutaneous tumors in the *SERPINE2*-knockdown group, sorafenib group, *SERPINE2*-knockdown + sorafenib group, and control group (mean  $\pm$  SD, unpaired Student's *t*-test). (H) Immunohistochemical staining of Ki-67 in the *SERPINE2*-knockdown group, sorafenib group, *SERPINE2*-knockdown + sorafenib group, and control group. (I) Patient-derived tumor culture flowchart. (J) Immunohistochemical staining of *SERPINE2* in patient-low and patient-high groups. (K-L) PDXs (K) and PDOs (L) from patients with low *SERPINE2* expression levels were more sensitive to sorafenib (Sora) than patients with high *SERPINE2* expression levels. \**P* < 0.05, \*\**P* < 0.01, \*\*\**P* < 0.001, \*\*\*\**P* < 0.0001. Abbreviations: EGFR, epidermal growth factor receptor; IC<sub>50</sub>, lower half-maximal inhibitory concentration; PDO, patient-derived organoid; PDX, patient-derived xenograft; SD, standard deviation; *SERPINE2*, serpin family E member 2; sh-Ctrl, sh-Control; Sora, sorafenib.

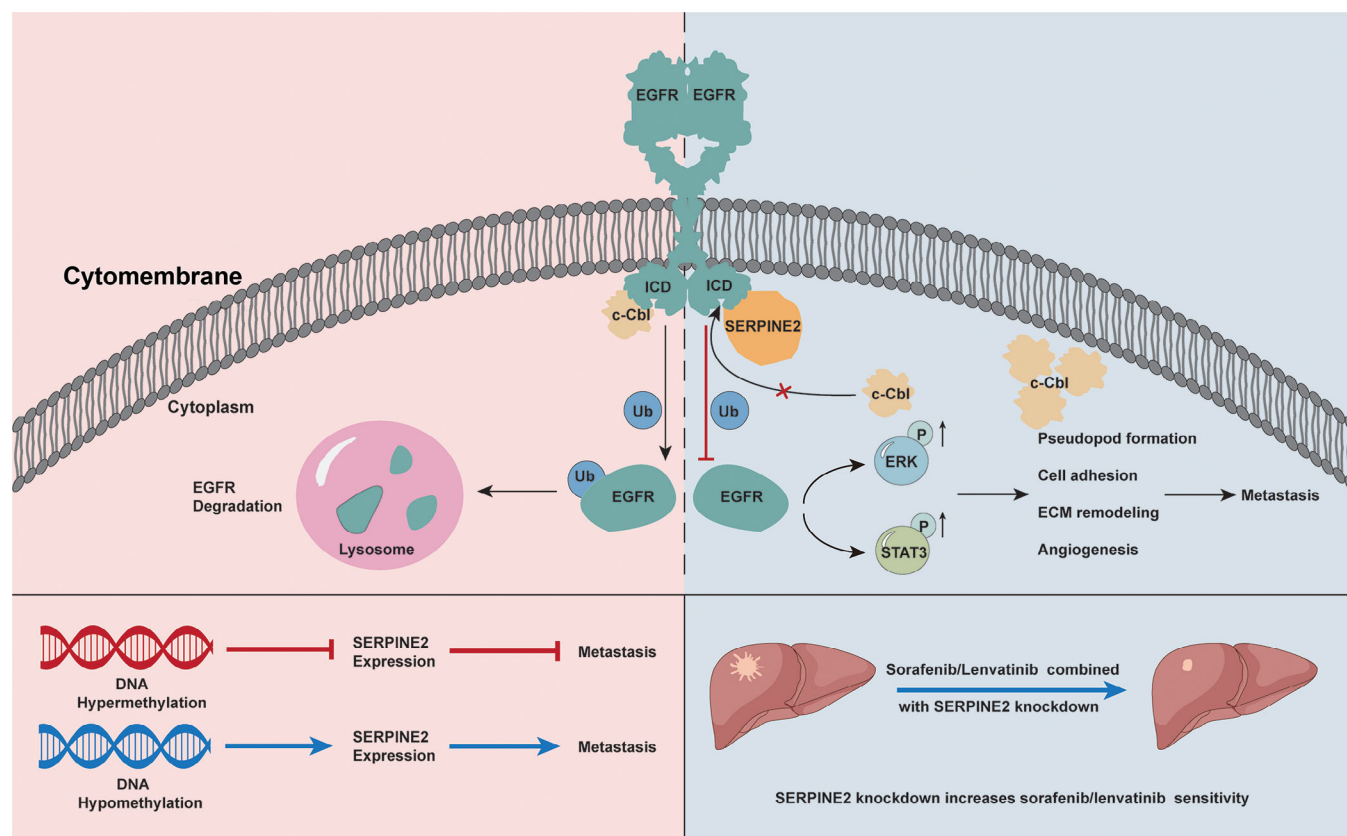


**FIGURE 8** Graphical schematic shows the role of *SERPINE2* in liver cancer metastasis. *SERPINE2* competes with c-Cbl for binding EGFR and stabilizes EGFR protein in liver cancer cells, which promotes the activation of STAT3 and ERK1/2 signaling pathways, leading to liver cancer cell migration and invasion, ECM remodeling and angiogenesis, and ultimately promotes liver cancer metastasis (upper panel). *SERPINE2* expression is regulated by DNA methylation (lower left panel), and *SERPINE2* knockdown can increase the sensitivity of liver cancer cells to sorafenib/lenvatinib (lower right panel). Abbreviations: c-Cbl, c-casitas B-lineage lymphoma; ECM, extracellular matrix; EGFR, epidermal growth factor receptor; ERK, extracellular regulated MAP kinase; ICD, intracellular domain; P, phosphorylation; *SERPINE2*, serpin family E member 2; STAT3, signal transducer and activator of transcription 3; Ub, ubiquitin.



processes by providing structural and growth factor support, anchoring cell adhesion, and inducing intracellular signaling pathways [38, 39]. CAFs are the most important component of the tumor microenvironment. Activated CAFs can promote tumor development and ECM remodeling through multiple pathways [40, 41]. It has been reported that overexpression of SERPINE2 in pancreatic tumors significantly promotes tumor invasion and the production of ECM in tumor tissues [42]. Our results confirmed that ECM- and CAF-related genes were significantly downregulated following SERPINE2 knockdown. Moreover, using a cell co-culture system, we found that the migration and adhesion abilities of CAFs were significantly inhibited after SERPINE2 knockdown, and the cytokine assays further confirmed that SERPINE2 promoted CAFs activation through TGF- $\beta$  secretion, suggesting that SERPINE2 is closely related to ECM and CAFs regulation.

EGFR is an important oncogene in various tumors, such as breast and non-small cell lung cancers [43]. In a previous study, 50 of 76 (66%) liver cancer tissue samples showed moderate-to-high EGFR expression levels [44]. Activation of EGFR and its downstream signaling pathway are closely related to liver cancer metastasis [45]. Rescue assays have confirmed that SERPINE2 mediated tumor metastasis by promoting EGFR expression in liver cancer. Furthermore, mass spectrometry and IP analysis revealed an interaction between SERPINE2 and EGFR and confirmed that SERPINE2 interacts with the ICD of EGFR. Ubiquitin and its related ubiquitin ligases play important roles in the precise regulation of key genes in all important biological processes, and dysregulation of ubiquitination may lead to tumorigenesis [46]. Ubiquitination of EGFR is a post-translational modification that regulates EGFR levels and activity. Dysregulation of EGFR ubiquitination has been implicated in the development and progression of various cancers, including liver cancer [47]. Ubiquitin analysis revealed that SERPINE2 significantly inhibited EGFR ubiquitination, thereby maintaining EGFR protein stability. EGFR ubiquitination plays an important role in the pathogenesis of liver cancer, and targeting this pathway may have therapeutic implications for the treatment of liver cancer.

c-Cbl, a member of the RING family, is normally expressed in cells. Previous studies have confirmed that c-Cbl is involved in signal transduction and has E3 ubiquitin ligase activity [48]. As a classical E3 ubiquitin ligase of EGFR, c-Cbl participates in EGFR internalization and degradation [49]. Previous studies have shown that c-Cbl can be directly recruited to Tyr1045 of the ICD to promote ubiquitination [14, 29], and IP assays confirmed that the binding ability of c-Cbl to EGFR was weakened when the Tyr1045 site of the ICD was mutated, which also attenu-

ated c-Cbl-mediated ubiquitination and the degradation of EGFR. However, the potential relationship between c-Cbl and SERPINE2 is still not fully understood, and further studies are required to determine the precise interactions between c-Cbl and SERPINE2 in liver cancer. Of note, the results of the IP assay showed that consistent with the findings for c-Cbl, SERPINE2 also binds to Tyr1045 of the ICD. Furthermore, we found that SERPINE2 overexpression significantly inhibited the interaction between c-Cbl and EGFR in a dose-dependent manner. These results suggest that SERPINE2 interacts with EGFR to attenuate c-Cbl-mediated EGFR ubiquitination and degradation.

Sorafenib is considered as a standard first-line agent for advanced liver cancer [50]; however, the insensitivity of some patients to sorafenib limits its efficacy [11]. Therefore, increasing the sensitivity to sorafenib is crucial for the treatment of liver cancer. The EGFR inhibitor erlotinib, alone or in combination with sorafenib, has shown some benefits in patients with liver cancer [51, 52]. Inhibitors of the EGFR and sorafenib enable a coordinated regulation of the RAF-MEK-ERK kinase cascade in liver cancer cells and increase sensitivity to sorafenib treatment [53]. Additionally, sorafenib alone inhibited phosphorylation of STAT3, while maintaining or even increasing phospho-ERK and/or phospho-AKT levels. However, the effects of sorafenib were prevented by gefitinib [54]. Moreover, hypoxia-inducible factor-2 $\alpha$  (HIF-2 $\alpha$ ) is considered to be the preferred target for individualized liver cancer therapy and sorafenib resistance. HIF-2 $\alpha$  activation subsequently leads to enhanced activation of VEGF, cyclin D1, and TGF- $\alpha$ /EGFR pathways, which mediate liver cancer development and reduce sorafenib sensitivity [55]. EGFR inhibitors block the TGF- $\alpha$ /EGFR pathway and reduce the activation of STAT3, AKT, and ERK, which synergistically inhibit the proliferation and induce the apoptosis of liver cancer cells treated with sorafenib [31]. Thus, we investigated whether EGFR downregulation caused by SERPINE2 knockdown plays an important role in increasing sorafenib sensitivity. Interestingly, SERPINE2 knockdown significantly reduced the IC<sub>50</sub> value of sorafenib in liver cancer cells. Furthermore, we demonstrated that SERPINE2 knockdown enhanced the pro-apoptotic effects of sorafenib in liver cancer cells. Therefore, we hypothesized that SERPINE2 knockdown increased the sensitivity of liver cancer cells to sorafenib by inhibiting the EGFR signaling pathway. Furthermore, lenvatinib is another first-line therapeutic agent for patients with advanced liver cancer, and it was reported that the level of phospho-EGFR was significantly upregulated in liver cancer cells after lenvatinib treatment [33]. Consistent with our hypothesis, we found that SERPINE2 knockdown can also increase lenvatinib sensitivity.

However, our study also has some limitations, such as the absence of clinical or preclinical targeting agents against SERPINE2. In recent years, there are been therapeutic strategies for targeted tumor therapy with siRNA encapsulated by nanocarriers [56, 57], which is worthy of further exploration. In addition, we found that the expression of SERPINE2 was upregulated after sorafenib treatment in our study. Further exploration of the mechanism of SERPINE2 upregulation after sorafenib treatment in the next study may provide further insights into the role of SERPINE2 in sorafenib resistance.

## 5 | CONCLUSIONS

We identified *SERPINE2* as a novel metastasis-promoting gene regulated by DNA methylation in liver cancer. SERPINE2 promoted the metastasis of liver cancer cells by inhibiting EGFR ubiquitination and maintaining EGFR protein stability. We also demonstrated the interaction between SERPINE2 and EGFR. We further explored the potential mechanism by which SERPINE2 competed with c-Cbl to bind to EGFR. Moreover, SERPINE2 knockdown significantly increased the sensitivity of liver cancer cells to sorafenib and lenvatinib. Therefore, the SERPINE2-EGFR axis may be a promising therapeutic target for liver cancer treatment.

## DECLARATIONS

### AUTHOR CONTRIBUTIONS

Shiyu Zhang: conceptualization, data curation, formal analysis, investigation, methodology, writing-original draft, and project administration. Xing Jia and Haojiang Dai: validation, investigation, methodology, project administration, writing-review, and editing. Xingxin Zhu and Wenfeng Song: data curation, formal analysis, supervision, and validation. Suchen Bian and Hao Wu: investigation, writing-review, and editing. Shinuo Chen, Yangbo Tang, and Junran Chen: validation and investigation. Cheng Jin and Mengqiao Zhou: investigation. Haiyang Xie: supervision, writing-review, and editing. Shusen Zheng and Penghong Song: conceptualization, resources, supervision, funding acquisition, writing-review, and editing.

## ACKNOWLEDGEMENTS

This work was supported by grants from the National Natural Science Foundation of China (82070652 and 81870434), the Department of Science and Technology of Zhejiang Province (2020C04003), the Chinese Academy of Medical Sciences (019-I2M-5-030), the Jinan Microecological Biomedicine Shandong Laboratory (JNL-2022007B), and

the State Key Laboratory for Diagnosis and Treatment of Infectious Diseases (zz202302).

## CONFLICT OF INTEREST STATEMENT

The authors declare that they have no competing interests.

## DATA AVAILABILITY STATEMENT

The data generated in this study are available within the article and its supplementary data files. The RNA sequencing data of liver cancer and paired adjacent normal tissues generated in this study are available upon reasonable request from the corresponding author.

## ETHICS APPROVAL AND CONSENT TO PARTICIPATE

All tissue samples were obtained from patients with liver cancer who underwent surgery at the First Affiliated Hospital of Zhejiang University School of Medicine. Written informed consent was obtained from each patient. This study was approved by the Ethics Committee of the First Affiliated Hospital of Zhejiang University School of Medicine (Ethics Code 2021-384). All animal experiments were approved by the Animal Care Committee of Zhejiang University (Ethics Code 2019-1218) and were conducted in strict accordance with the National Institutes of Health Animal Care and Use Guidelines.

## CONSENT FOR PUBLICATION

Not applicable.

## ORCID

Shusen Zheng  <https://orcid.org/0000-0003-1459-8261>

Penghong Song  <https://orcid.org/0000-0002-5167-1344>

## REFERENCES

1. Llovet JM, Kelley RK, Villanueva A, Singal AG, Pikarsky E, Roayaie S, et al. Hepatocellular carcinoma. *Nat Rev Dis Primers*. 2021;7(1):6.
2. Jiang H, Cao H-J, Ma N, Bao W-D, Wang J-J, Chen T-W, et al. Chromatin remodeling factor ARID2 suppresses hepatocellular carcinoma metastasis via DNMT1-Snail axis. *Proc Natl Acad Sci USA*. 2020;117(9):4770-80.
3. Ge T, Gu X, Jia R, Ge S, Chai P, Zhuang A, et al. Crosstalk between metabolic reprogramming and epigenetics in cancer: updates on mechanisms and therapeutic opportunities. *Cancer Commun (Lond)*. 2022;42(11):1049-82.
4. Song G, Zhu X, Xuan Z, Zhao L, Dong H, Chen J, et al. Hypermethylation of GNA14 and its tumor-suppressive role in hepatitis B virus-related hepatocellular carcinoma. *Theranostics*. 2021;11(5):2318-33.
5. Bouton M-C, Boulaftali Y, Richard B, Arocas V, Michel J-B, Jandrot-Perrus M. Emerging role of serpinE2/protease nexin-1 in hemostasis and vascular biology. *Blood*. 2012;119(11):2452-7.

6. Zou G, Lv Y, Kong M, Xiang B, Chen J. Upregulation of SERPINE2 Results in Poor Prognosis of Hepatoblastoma via Promoting Invasion Abilities. *Dis Markers*. 2022;2022:2283541.
7. Chen W-J, Dong K-Q, Pan X-W, Gan S-S, Xu D, Chen J-X, et al. Single-cell RNA-seq integrated with multi-omics reveals SERPINE2 as a target for metastasis in advanced renal cell carcinoma. *Cell Death Dis*. 2023;14(1):30.
8. Zhang J, Luo A, Huang F, Gong T, Liu Z. SERPINE2 promotes esophageal squamous cell carcinoma metastasis by activating BMP4. *Cancer Lett*. 2020;469:390-8.
9. Sasahira T, Kurihara-Shimomura M, Shimomura H, Kirita T. SERPINE2 is an oral cancer-promoting factor that induces angiogenesis and lymphangiogenesis. *Int J Clin Oncol*. 2021;26(10):1831-9.
10. Chong CR, Jänne PA. The quest to overcome resistance to EGFR-targeted therapies in cancer. *Nat Med*. 2013;19(11):1389-400.
11. Luo J, Li L, Zhu Z, Chang B, Deng F, Wang D, et al. Fucoidan inhibits EGFR redistribution and potentiates sorafenib to overcome sorafenib-resistant hepatocellular carcinoma. *Biomed Pharmacother*. 2022;154:113602.
12. Tomas A, Futter CE, Eden ER. EGF receptor trafficking: consequences for signaling and cancer. *Trends Cell Biol*. 2014;24(1):26-34.
13. Zhao L, Qiu T, Jiang D, Xu H, Zou L, Yang Q, et al. SGCE Promotes Breast Cancer Stem Cells by Stabilizing EGFR. *Adv Sci (Weinh)*. 2020;7(14):1903700.
14. Zhao X-C, Wang G-Z, Wen Z-S, Zhou Y-C, Hu Q, Zhang B, et al. Systematic identification of CDC34 that functions to stabilize EGFR and promote lung carcinogenesis. *EBioMedicine*. 2020;53:102689.
15. Shen H, He M, Lin R, Zhan M, Xu S, Huang X, et al. PLEK2 promotes gallbladder cancer invasion and metastasis through EGFR/CCL2 pathway. *J Exp Clin Cancer Res*. 2019;38(1):247.
16. Yang C, Zhang H, Zhang L, Zhu AX, Bernards R, Qin W, et al. Evolving therapeutic landscape of advanced hepatocellular carcinoma. *Nat Rev Gastroenterol Hepatol*. 2023;20(4):203-22.
17. Ji L, Lin Z, Wan Z, Xia S, Jiang S, Cen D, et al. miR-486-3p mediates hepatocellular carcinoma sorafenib resistance by targeting FGFR4 and EGFR. *Cell Death Dis*. 2020;11(4):250.
18. Arechederra M, Bazai SK, Abdouni A, Sequera C, Mead TJ, Richelme S, et al. ADAMTSL5 is an epigenetically activated gene underlying tumorigenesis and drug resistance in hepatocellular carcinoma. *J Hepatol*. 2021;74(4):893-906.
19. Pang L, Xu L, Yuan C, Li X, Zhang X, Wang W, et al. Activation of EGFR-KLF4 positive feedback loop results in acquired resistance to sorafenib in hepatocellular carcinoma. *Mol Carcinog*. 2019;58(11):2118-26.
20. Lai H-Y, Tsai H-H, Yen C-J, Hung L-Y, Yang C-C, Ho C-H, et al. Metformin Resensitizes Sorafenib-Resistant HCC Cells Through AMPK-Dependent Autophagy Activation. *Front Cell Dev Biol*. 2020;8:596655.
21. Pan X, Li J, Du W, Yu X, Zhu C, Yu C, et al. Establishment and characterization of immortalized human hepatocyte cell line for applications in bioartificial livers. *Biotechnol Lett*. 2012;34(12):2183-90.
22. Yang Z, Zhang L, Zhu H, Zhou K, Wang H, Wang Y, et al. Nanoparticle formulation of mycophenolate mofetil achieves enhanced efficacy against hepatocellular carcinoma by targeting tumour-associated fibroblast. *J Cell Mol Med*. 2021;25(7):3511-23.
23. Dong H, Li Z, Bian S, Song G, Song W, Zhang M, et al. Culture of patient-derived multicellular clusters in suspended hydrogel capsules for pre-clinical personalized drug screening. *Bioactive Materials*. 2022;18:164-77.
24. Winkler J, Abisoye-Ogunniyan A, Metcalf KJ, Werb Z. Concepts of extracellular matrix remodelling in tumour progression and metastasis. *Nat Commun*. 2020;11(1):5120.
25. Song M, He J, Pan Q-Z, Yang J, Zhao J, Zhang Y-J, et al. Cancer-Associated Fibroblast-Mediated Cellular Crosstalk Supports Hepatocellular Carcinoma Progression. *Hepatology*. 2021;73(5):1717-35.
26. Fang Z, Meng Q, Xu J, Wang W, Zhang B, Liu J, et al. Signaling pathways in cancer-associated fibroblasts: recent advances and future perspectives. *Cancer Commun (Lond)*. 2023;43(1):3-41.
27. Wu T, Wang W, Shi G, Hao M, Wang Y, Yao M, et al. Targeting HIC1/TGF- $\beta$  axis-shaped prostate cancer microenvironment restrains its progression. *Cell Death Dis*. 2022;13(7):624.
28. Xia J, Zhang S, Zhang R, Wang A, Zhu Y, Dong M, et al. Targeting therapy and tumor microenvironment remodeling of triple-negative breast cancer by ginsenoside Rg3 based liposomes. *J Nanobiotechnology*. 2022;20(1):414.
29. Grøvdal LM, Stang E, Sorkin A, Madhus IH. Direct interaction of Cbl with pTyr 1045 of the EGF receptor (EGFR) is required to sort the EGFR to lysosomes for degradation. *Exp Cell Res*. 2004;300(2):388-95.
30. Liu Y, Kong W-Y, Yu C-F, Shao Z-L, Lei Q-C, Deng Y-F, et al. SNS-023 sensitizes hepatocellular carcinoma to sorafenib by inducing degradation of cancer drivers SIX1 and RPS16. *Acta Pharmacol Sin*. 2023;44(4):853-64.
31. Zhao D, Zhai B, He C, Tan G, Jiang X, Pan S, et al. Upregulation of HIF-2 $\alpha$  induced by sorafenib contributes to the resistance by activating the TGF- $\alpha$ /EGFR pathway in hepatocellular carcinoma cells. *Cell Signalling*. 2014;26(5):1030-9.
32. Song W, Zheng C, Liu M, Xu Y, Qian Y, Zhang Z, et al. TRERNA1 upregulation mediated by HBx promotes sorafenib resistance and cell proliferation in HCC via targeting NRAS by sponging miR-22-3p. *Mol Ther*. 2021;29(8):2601-16.
33. Jin H, Shi Y, Lv Y, Yuan S, Ramirez CFA, Lieftink C, et al. EGFR activation limits the response of liver cancer to lenvatinib. *Nature*. 2021;595(7869):730-4.
34. Mattei AL, Bailly N, Meissner A. DNA methylation: a historical perspective. *Trends Genet*. 2022;38(7):676-707.
35. Nishiyama A, Nakanishi M. Navigating the DNA methylation landscape of cancer. *Trends Genet*. 2021;37(11):1012-27.
36. Irizarry RA, Ladd-Acosta C, Wen B, Wu Z, Montano C, Onyango P, et al. The human colon cancer methylome shows similar hypo- and hypermethylation at conserved tissue-specific CpG island shores. *Nat Genet*. 2009;41(2):178-86.
37. Zhu X, Song G, Zhang S, Chen J, Hu X, Zhu H, et al. Asialoglycoprotein Receptor 1 Functions as a Tumor Suppressor in Liver Cancer via Inhibition of STAT3. *Cancer Res*. 2022;82(21):3987-4000.
38. Huang J, Zhang L, Wan D, Zhou L, Zheng S, Lin S, et al. Extracellular matrix and its therapeutic potential for cancer treatment. *Signal Transduct Target Ther*. 2021;6(1):153.
39. Jiang Y, Zhang H, Wang J, Liu Y, Luo T, Hua H. Targeting extracellular matrix stiffness and mechanotransducers to improve cancer therapy. *J Hematol Oncol*. 2022;15(1):34.



40. Mao X, Xu J, Wang W, Liang C, Hua J, Liu J, et al. Crosstalk between cancer-associated fibroblasts and immune cells in the tumor microenvironment: new findings and future perspectives. *Mol Cancer*. 2021;20(1):131.
41. Asif PJ, Longobardi C, Hahne M, Medema JP. The Role of Cancer-Associated Fibroblasts in Cancer Invasion and Metastasis. *Cancers*. 2021;13(18):4720.
42. Buchholz M, Biehl A, Neesse A, Wagner M, Iwamura T, Leder G, et al. SERPINE2 (protease nexin I) promotes extracellular matrix production and local invasion of pancreatic tumors in vivo. *Cancer Res*. 2003;63(16):4945-51.
43. Ji X, Chen X, Zhang B, Xie M, Zhang T, Luo X, et al. T-box transcription factor 19 promotes hepatocellular carcinoma metastasis through upregulating EGFR and RAC1. *Oncogene*. 2022;41(15):2225-38.
44. Buckley AF, Burgart LJ, Sahai V, Kakar S. Epidermal growth factor receptor expression and gene copy number in conventional hepatocellular carcinoma. *Am J Clin Pathol*. 2008;129(2):245-51.
45. Ueno S, Mojic M, Ohashi Y, Higashi N, Hayakawa Y, Irimura T. Asialoglycoprotein receptor promotes cancer metastasis by activating the EGFR-ERK pathway. *Cancer Res*. 2011;71(20):6419-27.
46. Cruz Walma DA, Chen Z, Bullock AN, Yamada KM. Ubiquitin ligases: guardians of mammalian development. *Nat Rev Mol Cell Biol*. 2022;23(5):350-67.
47. Li K-S, Zhu X-D, Liu H-D, Zhang S-Z, Li X-L, Xiao N, et al. NT5DC2 promotes tumor cell proliferation by stabilizing EGFR in hepatocellular carcinoma. *Cell Death Dis*. 2020;11(5):335.
48. Hou J, Xu M, Gu H, Pei D, Liu Y, Huang P, et al. ZC3H15 promotes glioblastoma progression through regulating EGFR stability. *Cell Death Dis*. 2022;13(1):55.
49. Visser Smit GD, Place TL, Cole SL, Clausen KA, Vemuganti S, Zhang G, et al. Cbl controls EGFR fate by regulating early endosome fusion. *Sci Signal*. 2009;2(102):ra86.
50. Tang W, Chen Z, Zhang W, Cheng Y, Zhang B, Wu F, et al. The mechanisms of sorafenib resistance in hepatocellular carcinoma: theoretical basis and therapeutic aspects. *Signal Transduct Target Ther*. 2020;5(1):87.
51. Philip PA, Mahoney MR, Allmer C, Thomas J, Pitot HC, Kim G, et al. Phase II study of Erlotinib (OSI-774) in patients with advanced hepatocellular cancer. *J Clin Oncol*. 2005;23(27):6657-63.
52. Zhu AX, Rosmorduc O, Evans TRJ, Ross PJ, Santoro A, Carrilho FJ, et al. SEARCH: a phase III, randomized, double-blind, placebo-controlled trial of sorafenib plus erlotinib in patients with advanced hepatocellular carcinoma. *J Clin Oncol*. 2015;33(6):559-66.
53. Ezzoukhry Z, Louandre C, Trécherel E, Godin C, Chauffert B, Dupont S, et al. EGFR activation is a potential determinant of primary resistance of hepatocellular carcinoma cells to sorafenib. *Int J Cancer*. 2012;131(12):2961-9.
54. Blivet-Van Eggelpoël M-J, Chettouh H, Fartoux L, Aoudjehane L, Barbu V, Rey C, et al. Epidermal growth factor receptor and HER-3 restrict cell response to sorafenib in hepatocellular carcinoma cells. *J Hepatol*. 2012;57(1):108-15.
55. Dong X-F, Liu T-Q, Zhi X-T, Zou J, Zhong J-T, Li T, et al. COX-2/PGE2 Axis Regulates HIF2 $\alpha$  Activity to Promote Hepatocellular Carcinoma Hypoxic Response and Reduce the Sensitivity of Sorafenib Treatment. *Clin Cancer Res*. 2018;24(13):3204-16.
56. Zheng M, Liu Y, Wang Y, Zhang D, Zou Y, Ruan W, et al. ROS-Responsive Polymeric siRNA Nanomedicine Stabilized by Triple Interactions for the Robust Glioblastoma Combinational RNAi Therapy. *Adv Mater*. 2019;31(37):e1903277.
57. Zhuang J, Gong H, Zhou J, Zhang Q, Gao W, Fang RH, et al. Targeted gene silencing in vivo by platelet membrane-coated metal-organic framework nanoparticles. *Sci Adv*. 2020;6(13):eaaz6108.

## SUPPORTING INFORMATION

Additional supporting information can be found online in the Supporting Information section at the end of this article.

**How to cite this article:** Zhang S, Jia X, Dai H, Zhu X, Song W, Bian S, et al. SERPINE2 promotes liver cancer metastasis by inhibiting c-Cbl-mediated EGFR ubiquitination and degradation. *Cancer Commun*. 2024;1–24. <https://doi.org/10.1002/cac2.12527>